

Experimental Investigation on Self-Compacting Fiber Reinforced Concrete Slabs

Orod Zarrinkafsh

Submitted to the
Institute of Graduate Studies and Research
in the partial fulfillment of the requirements for the Degree of

Master of Science
in
Civil Engineering

Eastern Mediterranean University
February 2015
Gazimağusa, North Cyprus

Approval of the Institute of Graduate Studies and Research

Prof. Dr. Serhan Çiftçiođlu
Director

I certify that this thesis satisfies the requirements of thesis for the degree of Master of Science in Civil Engineering.

Prof. Dr. Özgür Eren
Chair, Department of Civil Engineering

We certify that we have read this thesis and that in our opinion it is fully adequate in scope and quality as a thesis for the degree of Master of Science in Civil Engineering.

Prof. Dr. Özgür Eren
Co-supervisor

Asst. Prof. Dr. Serhan Şensoy
Supervisor

Examining Committee

1. Prof. Dr. Özgür Eren

2. Asst. Prof. Dr. Tülin Akçaođlu

3. Asst. Prof. Dr. Mürüde Çelikađ

4. Asst. Prof. Dr. Giray Ozay

5. Asst. Prof. Dr. Serhan Şensoy

ABSTRACT

The purpose of this thesis is to determine the effect of steel fibers on mechanical performance of traditionally reinforced self-compacting concrete (SCC) slabs. The design is based on flexural failure; subsequently the dimensions of slabs are determined to prevent shear failure.

In this study, slabs designed for concrete classes of C20 and C40 with self-compacting concrete in the dimensions of 2200×300×200 mm were tested. For each type of mix, four different volume percentages of 60/30 (length/diameter) fiber (0.0%, 1.0%, 1.5% and 2%) were used and it provided a total of 14 types of slab models.

For these tests, an IPE 400 was used by two shafts beneath it for dividing the load in two equal parts. Data Logger machine was used to crack the slabs by applying the two point load in the middle of the slab. During the test, 4 strain sensors were placed at the top and bottom of each slab and also a transducer was placed at the bottom center of it.

According to the experimental tests which have been made in this investigation, the result revealed that fibers can improve some properties of self-compacting concrete such as flexural strength and enhance mechanical performance. By performing flexural tests, slabs behavior were improved due to fiber influence on energy absorption and flexural behavior. The results clearly showed that the use of fiber can improve the post-cracking behavior. And also, fiber can increase the tensile strength

by bridging through the cracks. Therefore, steel fibers increase the ductility and energy absorption capacity of RC elements subjected to flexure.

Keywords: Self-Compacting Concrete, Steel Fibers, Flexural Strength, Reinforced Concrete, Energy Absorption Capacity.

ÖZ

Bu çalışmanın amacı betona karıştırılan çelik liflerin kendinden yerleşen betonda kullanılması ile üretilen kirişlerin mekanik özelliklerindeki değişikliklerin belirlenmesidir. Kirişlerin ve plakların boyutları ise betonun eğilme dayanımı ve kesme kuvvetleri esas alınarak tasarlanmıştır.

Tasarlanan beton sınıfı C20 ve C40 olarak düşünülmüş ve 2200x300x200 mm boyutlarındaki plakalar üretilmiştir. Her bir karışımda 60/30 narinlik oranına sahip tek tip ve dört değişik çelik lif hacmi (%0, %1, %1,5 ve %2) kullanılarak 14 değişik plaka üretilmiştir. Deney düzeneği için IPE400 çelik kiriş ve yükleri iki eşit noktaya dağıtmak amacı ile de iki Çelik silindir kullanıldı. Elde edilen yük, deplasman, birim deformasyonlar data kayıt edici kullanıldı.

Deney sırasında, dört adet deformasyon ölçen sensor kullanılarak plakanın üzerinden ve altından veri toplanmıştır. Elde edilen sonuçlara bakıldığında ise çelik liflerin kendinden yerleşen beton ile üretilen plakaların eğilme dayanımını ve betonun tokluk enerji emme kapasitesini iyileştirdiği görülmüştür. Bunun dışında yükleme sırasında çatlak oluşumunun da çelik liflerin etkisi ile geciktiği açıkça görülmüştür. Çelik lifler çatlaklar arasında köprü görevi görmekte ve çatlakların ilerlemesi durmaktadır.

Anahtar Kelimeler: kendinden yerleşen beton, çelik lif, eğilme dayanımı, betonarme betonu, tokluk enerjisi.

To My beloved Mother and Father

ACKNOWLEDGMENT

Foremost, I would like to express my sincere gratitude to my supervisor Assistant Professor Dr. Serhan Şensoy for the continuous support of my Master thesis study and research, for his patience, enthusiasm, and immense knowledge.

Also, I had a great opportunity to get help from Professor Dr. Özgür Eren and I acknowledge his advises for concrete mix-design. A special thanks to my dear mother and father for their constant help throughout my education.

And thanks to my friends Hassan Moniri, Mohammad Golhashem and Mohesn Ramezan Shirazi for their help my thesis.

TABLE OF CONTENTS

ABSTRACT.....	iii
ÖZ	v
ACKNOWLEDGMENT.....	vii
LIST OF TABLES.....	xi
LIST OF FIGURES.....	xii
1 INTRODUCTION	1
1.1 Background	1
1.2 Objective	4
1.3 Scope.....	4
1.4 Significance.....	4
2 BACKGROUND INFORMATION AND LITERATURE REVIEW.....	5
2.1 Introduction.....	5
2.2 Previous Studies.....	5
2.3 Mechanical Properties.....	8
2.3.1 Compressive Strength	8
2.3.2 Toughness Tests.....	10
2.3.3 Cracking Behavior	11
2.5 Mix Design for SFRC	16
2.5.1 Workability.....	16
2.5.2 Test of workability/consistency.....	16
2.6 Previous Studies	20
2.6.1 SFRC Constitutive Concept in Compression.....	20
2.6.2 Direct Tensile Tests	21

2.7 Crack Patterns	22
2.8 Toughness.....	27
3 METHODOLOGY.....	30
3.1 Introduction.....	30
3.2 Experimental Module.....	30
3.2.1 Specimens Provision	30
3.2.2 Evaluating of Required Load	32
3.2.3 Concrete and Mix Design.....	33
3.3 Sieve Analysis	34
3.4 Compressive Strength Test.....	37
3.5 Testing Fresh SCC.....	38
3.5.1 Slump Flow and T50 Test	38
3.5.2 L-box Test	39
3.5.2.1 Test Procedure	39
3.5.3 J-ring Test.....	40
3.5.3.1 Test Procedure	40
3.5.4 V-funnel Test.....	40
3.5.4.1 Test Procedure	41
3.4.1 Casting and Curing.....	42
3.5 Flexural Test Setup.....	43
3.5.1 Test Apparatus	43
4 ANALYSIS, RESULTS AND DISCUSSION.....	45
4.1 Results of T50, Slump, L-box, V-Funnel and J-Ring	45
4.2 Compressive Strength Test Results of Cubes.....	46
4.3 Experimental Results of Flexural Test	46

4.3.1 TDS Setup	46
4.3.2 Slab with Different Percentage of Fibers for C40 Concrete	48
4.3.2.1 Mixture of 2% Super plasticizer for - 0% Fibers	48
4.3.2.2 Mixture of 2% Super plasticizer for - 1% Fibers	50
4.3.2.3 Mixture of 2% Super plasticizer for – 1.5% Fibers	52
4.3.2.4 Mixture of 2% Super plasticizer for – 2% Fiber	53
4.3.2.5 Mixture of 1% Super plasticizer for – 0% Fibers	54
4.3.2.6 Mixture of 1% Super plasticizer for – 1% Fibers	55
4.3.2.7 Mixture of 1% Super plasticizer for – 1.5% Fibers	56
4.3.2.8 Mixture of 1% Super plasticizer for – 2% Fibers	57
4.3.2.9 Moment-Curvature Comparison of C20 and C40 Concrete	57
4.3.2.10 Load-Displacement Comparison of C20 and C40 Concrete.....	59
4.3.2.11 Stress Strain Relationship.....	60
5 CONCLUSION	66
5.1 Conclusions	66
5.2 Future Studies	67
REFERENCES.....	68

LIST OF TABLES

Table 1: SCC projects (Daczko, 2012) [16].....	2
Table 2: Test method description (Banthia, 2012) [39].....	11
Table 3: Concrete composition (dry materials) (Ding, 2012) [82].....	19
Table 4: Effect of fiber reinforcement on cracking observed at the failure level.....	23
Table 6: Steel fibers characteristics.....	33
Table 7: Sieve analysis for 20mm D_{max} of aggregate.....	35
Table 8: Sieve analysis for 14 mm D_{max} of aggregate.....	35
Table 9: Sieve analysis for 10 mm of aggregate	35
Table 10: Sieve analysis for 5 mm of fine aggregate	36
Table 11: Sieve analysis for 5 mm of aggregate	36
Table 12: Mix design for C20 Concrete	37
Table 13: Mix design for C40 Concrete	37
Table 14: Compressive strength test results for cube samples of C20.....	38
Table 15: Compressive strength test results for cube samples of C40.....	38
Table 16: Workability test results of Self-Compacting Concrete.....	45
Table 17: Compressive strength results of cubes (MPa).....	46
Table 18: Energy absorption	60

LIST OF FIGURES

Figure 1: Hooked-end steel fibers (Lachemi <i>et al.</i> 2013)	4
Figure 2: Effect of fibers and failure mechanism (Nataraja, 2011).....	6
Figure 3: VeBe time vs fiber content with different sizes of aggregate (Endgington <i>et al.</i> 1974)	7
Figure 4: Effect of aspect ratio of fiber on compacting factor (Endgington <i>et al.</i> 1974)	7
Figure 5: Stress-Strain curves in compression for SFRC (Johnston, 1997).....	8
Figure 6: SFRC before and after appearing of crack bridging (right) and macro crack (left) (Banthia, 2012).....	9
Figure 7: Crack of plastic shrinkage (left) and crack width (right) (Banthia, 2012) .	10
Figure 8: Crack pattern (Vandewalle, 2000)	12
Figure 9: Average crack spacing (Vandewalle, 2000).....	12
Figure 10: Distribution of stress in cracked section. (Vandewalle, 2000)	14
Figure 11: Tensile stress calculation (Vandewalle, 2000)	14
Figure 12: Relationship, between inverted cone time, VeBe time and slump (Nataraja, 2011).....	17
Figure 13: VeBe time vs fibers percentage (Nataraja, 2011)	17
Figure 14: Average Load-Deflection at the mid-span (Soltanzadeh <i>et al.</i> 2013).....	18
Figure 15: Crack opening versus residual post-peak strength crack opening in a direct tensile test on notched specimen (Fritih, 2013)	21
Figure 16: Crack pattern and loading levels on beams (Fritih <i>et al.</i> 2013).....	23
Figure 17: Failure and crack pattern of beams with 0.22% stirrup ratio (Ding <i>et al.</i> 2012)	25

Figure 18: Comparison of local stresses at a crack with calculated average stresses of SFRC and stress state of a single fiber (Ding <i>et al.</i> 2012)	27
Figure 19: Load vs deflection responses in beams with diverse stirrup ratios (Ding <i>et al.</i> 2012)	28
Figure 20: Increase of toughness factor for beams with various reinforcements (Ding <i>et al.</i> 2012)	29
Figure 21: IPE and slab deformation	31
Figure 22: Dimensions of plate, shaft and IPE	31
Figure 23: Load capacity of SCC	32
Figure 24: Formwork construction and bars	34
Figure 25: Sieve analysis	34
Figure 26: Sieve analysis for coarse aggregate	36
Figure 27: Sieve analysis graph fine aggregate.....	37
Figure 28: Slump and T50 tests	39
Figure 29: L-box test.....	39
Figure 30: J-ring test	40
Figure 31: V funnel equipment	41
Figure 32: V funnel test.....	41
Figure 33: Slab formwork and steel bars	42
Figure 34: Slab filled with SCC	43
Figure 35: Test apparatus for flexural strength	44
Figure 36: Test apparatus (load cell and IPE 400)	47
Figure 37: Test apparatus (load cell, IPE400, and transducer).....	47
Figure 38: Load-Displacement diagram for C40 concrete (2%SP-0%Fiber)	48
Figure 39: Crack pattern for concrete C40 (2%SP-0%Fiber)	49

Figure 40: Moment-Curvature diagram for C40 concrete (2%SP - 0%Fiber).....	50
Figure 41: Load-Displacement diagram for C40 concrete (2%SP - 1%Fiber)	50
Figure 42: Crack section (2%SP - 1%Fiber).....	51
Figure 43: Load-Displacement diagram for C40 concrete (2%SP - 1%Fiber)	51
Figure 44: Load-Displacement diagram for C40 concrete (2%SP – 1.5%Fiber).....	52
Figure 45: Load-Displacement diagram for C40 concrete (2%SP – 1.5%Fiber).....	52
Figure 46: Load-Displacement diagram for C40 concrete (2%SP – 2%Fiber).....	53
Figure 47: Moment-Curvature diagram for C40 concrete (2%SP – 2%Fiber)	53
Figure 48: Load-Displacement diagram for C20 concrete (1%SP – 0%Fiber).....	54
Figure 49: Moment-Curvature diagram for C20 concrete (1%SP – 0%Fiber)	54
Figure 50: Load-Displacement diagram for C20 concrete (1%SP – 1%Fiber).....	55
Figure 51: Moment-Curvature diagram for C20 concrete (1%SP – 1%Fiber)	55
Figure 52: Load-Displacement diagram for C20 concrete (1%SP – 1.5%Fiber).....	56
Figure 53: Moment-Curvature diagram for C20 concrete (1%SP – 1.5%Fiber)	56
Figure 54: Load-Displacement diagram for C20 concrete (1%SP – 2%Fiber).....	57
Figure 55: Moment-Curvature diagram for C20 concrete (1%SP – 2%Fiber)	57
Figure 56: Moment-Curvature diagram C20.....	58
Figure 57: Moment-Curvature diagram C40.....	58
Figure 58: Load-Displacement diagram C20.....	59
Figure 59: Load-Displacement diagram C40.....	59
Figure 60: Load-Displacement diagram C20 and C40 0% Fiber.....	61
Figure 61: Load-Displacement diagram C20 and C40 1% Fiber.....	61
Figure 62: Load-Displacement diagram C20 and C40 1.5% Fiber.....	62
Figure 63: Load-Displacement diagram C20 and C40 2% Fiber.....	62
Figure 64: Core sample for Stress-Strain curvature.....	63

Figure 65: Stress-Strain curvature for C20	63
Figure 66: Stress-Strain curvature C40	64
Figure 67: Fibers for bridging cracks.....	65

LIST OF ABBREVIATIONS

FRC	Fibrous Reinforced Concrete
SFRC	Steel Fibrous Reinforced Concrete
SCC	Self Compacting Concrete
FRSCC	Fibrous Reinforced Self Compacting Concrete
HPFRC	High Performance Fiber Reinforced Concrete

LIST OF SYMBOLS

ρ	Tensile reinforcement ratio
f'_c	Compressive strength of concrete
l/d	Aspect ratio of fibers
v_f	Fiber amount of concrete
a/d	Ratio of span-depth
ϕ	Bar size
σ_s	Tension stress in reinforcement according to a cracked section
σ_{sr}	Tension stresses according to the first crack
δ	Deflection in pure bending zone
K_0	Corrected gauge factor
r	Total resistance of load wires
L	Length of load wires (m)
K	Gauge factor
R	Gauge resistance
C_s	Strain sensor coefficient

Chapter 1

INTRODUCTION

1.1 Background

Self-compacting concrete (SCC) doesn't need to vibrator, due to the compacting ability by its own weight without vibration. In addition, SCC can reduce construction time and labor cost (Hossain *et al.* 2013).

SCC has been developed in 1980s to overcome the steel bar congestion in active seismic regions (Ozawa *et al.* 1989). Researches on SCC continues through the last decades (Ozawa *et al.* 1989, Rols *et al.* 1999, Bui *et al.* 2002, Lachemi *et al.* 2003, Lachemi *et al.* 2004). The use of fibers in SCC improves the mechanical properties and durability of hardened concrete such as impact strength, flexural strength, and vulnerability to cracking, resistance to fatigue, toughness and spelling (ACI 544 1990, Nehdi *et al.* 2004, Tlemat *et al.* 2003, Malhotra *et al.* 1994, Nanni, 1988).

Initially, the idea of SCC appeared for using in inaccessible areas and underwater structures (Gaimster, & Dixon, 2003). Self-compacting concrete has been developed more in recent years, but total productions are still less than the conventional concrete (Sarmiento, 2010-2011). In Netherland, about 70% of precast concrete was SCC in 2005; however, this proportion in Denmark was just 30% of conventional concrete (Geiker, 2008).

Table 1 shows some of the projects that SCC was used. The SCC usage has varieties such as cast-in-place or precast, complicated buildings or simple, small or big structures, vertical or horizontal members (Yakhlaf, 2013).

In the U.S, the use of SCC is nearly 40% in precast production (Daczko, 2012). Recently, the usage of SCC widened to repair materials in Switzerland and Canada (ACI 237R-07 2007, EFNARC 2002).

Table 1: SCC projects (Daczko, 2012)

Location	Cast –in-place or Precast	Project	Volume of concrete (m³)
Japan	Cast –in-place	LNG storage tank	12,000
Japan	Cast –in-place	Water purification plant	200,000
Japan	Cast –in-place	MMST tunneling	8000
USA	Cast –in-place	National Museum of the American Indian	23,000
Canada		Reaction Wall, University of Sherbrook	
Korea	Cast –in-place	Diaphragm wall for in ground LNG tank	32,800
Canada	Cast –in-place	Fill abandoned pump station in mine	
USA	Cast –in-place	LNG storage tank	25,000
Italy	Cast –in-place	Foundations and slabs for housing	123,000
USA	Cast –in-place	Double tee production	
New Zealand	Cast –in-place	Precast beams	

The shear resistance of fiber reinforced concrete generally depends on tensile reinforcement ratio (ρ), compressive strength of concrete (f'_c), the ratio of span-depth (a/d), the fiber amount of concrete (v_f) and aspect ratio of fibers (l/d) (EFNARC 2002). Fibers provide further resistance against crack development by creating bridges through cracks (Narayanan, & Darwish, 1987, Li *et al.* 1992, Lim, & Oh, 1999). Therefore, steel fibers in the reinforced concrete change the behavior from brittle to ductile and increase the shear capacity (Mansur *et al.* 1986), (Ramakrishna, & Sundararajan, 2005). Limiting the tensile crack to a certain location and preventing of excessive diagonal tensile cracking are other advantages of steel fiber (Choi, & Park, 2007).

The advantages of both SCC and SFRC are gathered in FRSCC (Fiber-reinforced self-compacting concrete) which is a recent composite material. FRSCC can enhance two weaknesses: the workability which is effected by fibers in SFRC and increase the resistance against the crack in plain concrete (Aslani, & Nejadi, 2013). Fibers made of glass, carbon, plastic, polymer, and steel (Figure 1) or rubber can be used to produce FRC (Lachemi *et al.* 2013). The investigation has been leading to the development of SCC (FRSCC), which lead to the greater ductility, durability and mechanical features of FRC with the workability of ordinary SCC (Ozawa *et al.* 1989, Khayat *et al.* 2000, Ding *et al.* 2008, Sahmaran, *et al.* 2005, Aydin, 2007).



Figure 1: Hooked-end steel fibers (Lachemi *et al.* 2013)

1.2 Objective

In this research, the effect of different percentage of fibers on flexural behavior of the self-compacting concrete (SCC) slabs with a minimum longitudinal bar ratio has been investigated. Furthermore, effects of fibers on the energy absorption capacity of reinforced concrete slabs without any transverse reinforcement are examined to assess the enhancement of fiber utilization.

1.3 Scope

The slabs tested in this study have two different concrete classes namely C20 and C40 and have been designed according to ACI318-02 with different percentages of fibers 0.0, 1.0, 1.5 and 2.0 with length over diameter of 60/30. These samples are subjected to displacement-controlled load and stress-controlled load.

1.4 Significance

On this account, the characteristics of materials that can dissipate energy are one of the most important issues. This property is influenced by many different parameters like fiber that can improve the behavior of plain concrete by increasing ductility. In this investigation, enhancement of energy absorption due to different percentages of fibers is considered.

Chapter 2

BACKGROUND INFORMATION AND LITERATURE REVIEW

2.1 Introduction

Researches have been done on FRSCC (Fiber Reinforcement Self-Compacting Concrete) which can divide into two different fields, material serviceability and mechanical investigations. The mechanical aspect of FRSCC has been studied by several researchers to provide the constitutive models of shear and flexure capacity, tensile or compressive zone data. In this part, major studies on FRSCC are reviewed to prepare an adequate background of FRSCC (Pir, 2013).

2.2 Previous Studies

The fibers that are commercially used in civil engineering applications are steel (SFRC/SFRS), aramid, carbon and glass. The propagation of steel fibers promotes the controlling of micro-cracks. First they improve the overall resistance of the matrix and secondly by bridging through smaller cracks, thus decrease the growth of major cracks (Figure 2).

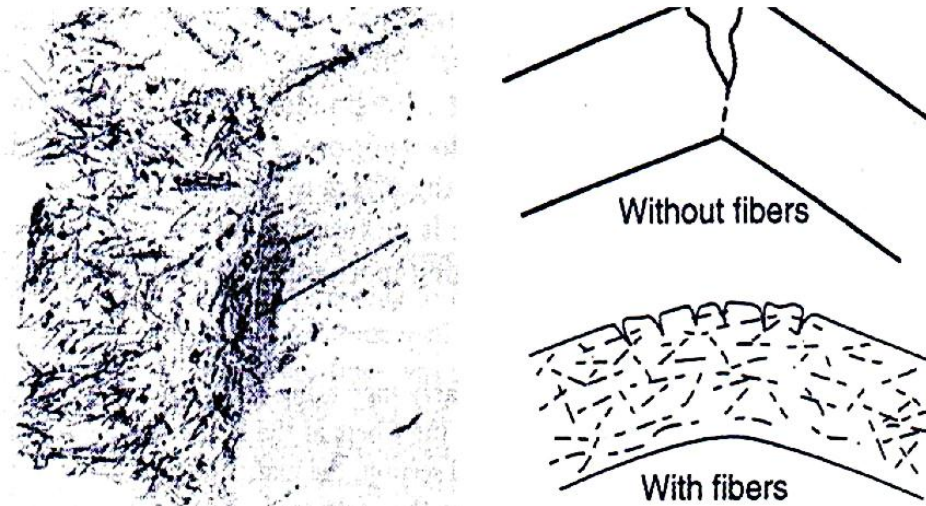


Figure 2: Effect of fibers and failure mechanism (Nataraja, 2011)

Researchers studied steel fiber self-compacting concrete (SFSCC) and fiber reinforced concrete (FRC) to find out the characteristics of post-cracking behavior and workability. By using SFSCC the costs and construction period reduces significantly and its ability to place irregular section in terms of congestion of stirrups and bars and thin section is another great aspect (Nataraja, 2011).

The consequence of this capability is to arrest cracks and, fiber in mixtures increased tensile strength, both at ultimate and at first crack, especially under flexural loading. The other ability of fibers is to hold a matrix after extensive cracking. The transition failure from brittle to ductile is another ability of fibers which can absorb energy and survive under impact loading.

The fibers types, percentage and orientation of fibers effects the workability, and the workability can be decreased by increasing the quantity and size of aggregate (greater than 5 mm). On the other hand, the aggregate less than 5 mm has little effect on mix compaction (Chanh, 2007). Figure 3 illustrates the effects of aggregate size on the VeBe time.

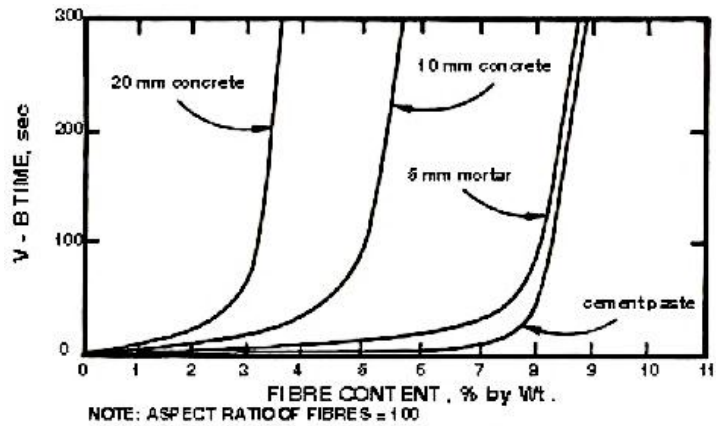


Figure 3: VeBe time vs fiber content with different sizes of aggregate (Endgington *et al.* 1974)

On the second stage, the aspect ratio of fibers has a key effect on the workability. The workability is reduced by the increasing aspect ratio. Figure 4 presented the effect of aspect ratio of fibers on the workability in terms of compacting factor.

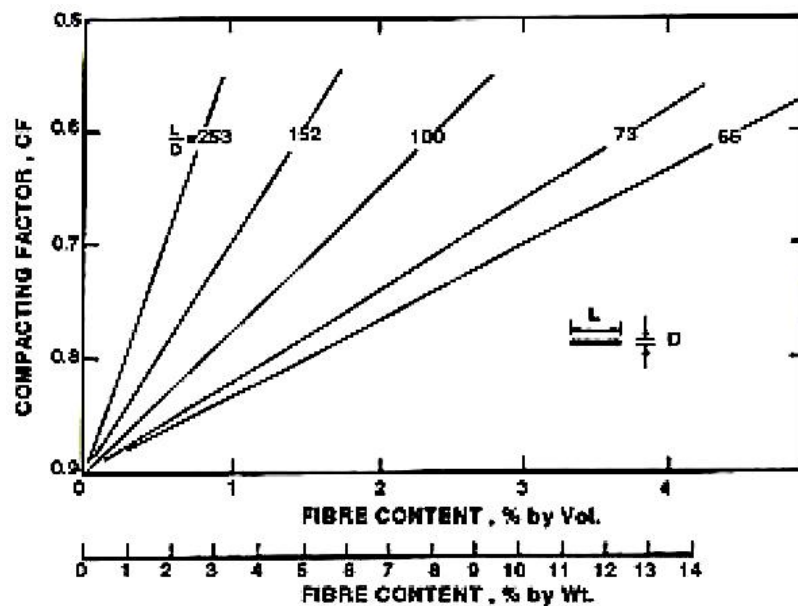


Figure 4: Effect of aspect ratio of fiber on compacting factor (Endgington *et al.* 1974)

One of the main problems to produce a uniform fiber distribution is the trend for fibers to clump or ball together. Clumping can be initiated by the following factors:

- The fibers might be clumped before adding to the mix and the normal mixing action cannot break down its clump.

- Fibers might be added quickly and doesn't allow scattering in the mixer.
- The high volume of fibers can cause clamping.

It is worth to mention that, adding water is only for improving the workability with great care. In the SFRC further water might increase the slump, without increasing its workability.

2.3 Mechanical Properties

2.3.1 Compressive Strength

Fibers have little influence through compressive strength. It increases the strength ranging from nil to 25%. But fibers significantly increase the energy absorption and ductility in post-cracking. You can see the SFRC stress-strain curves in Figure 5.

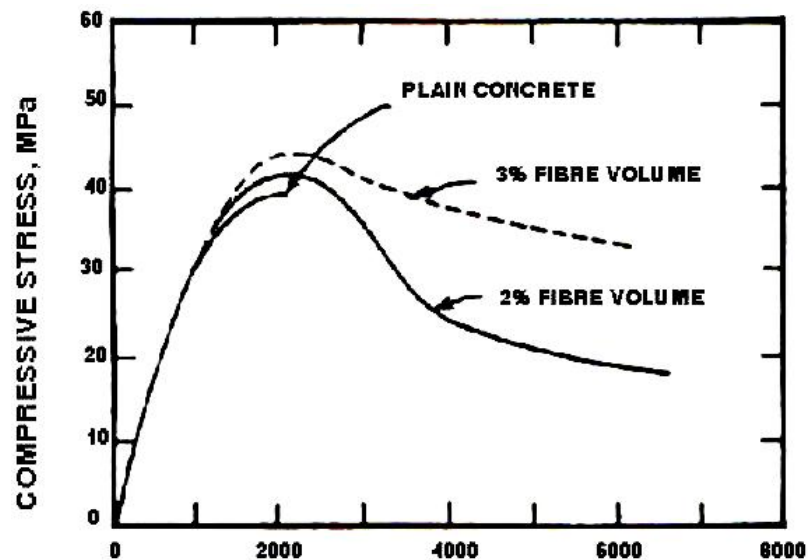


Figure 5: Stress-Strain curves in compression for SFRC (Johnston, 1997)

The factors that affect the shear capacity on the SFRC:

- Increase the ration of tensile reinforcement.
- The ratio of shear span-depth of the beam.
- Ultimate compressive strength (Alam, 2013)

By bonding fibers properly in hardened concrete, interact with the matrix at micro-cracks level and successfully bridge through the cracks can transfer stress and delay the unstable growth (Figure 6).

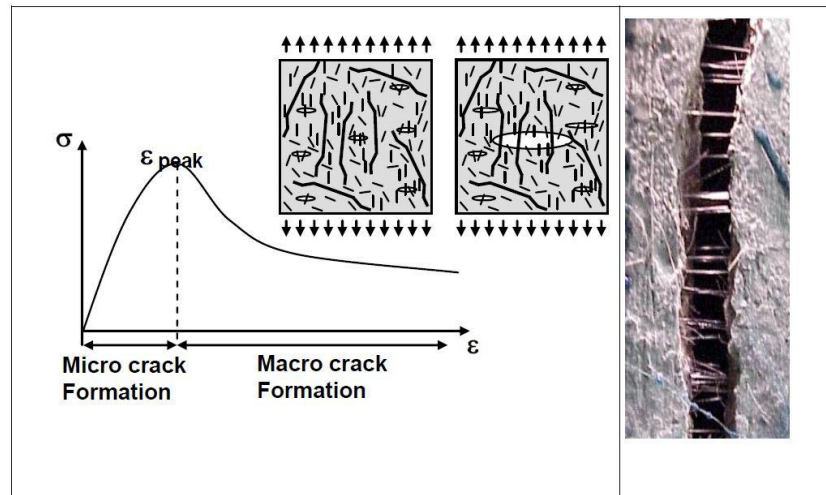


Figure 6: SFRC before and after appearing of crack bridging (right) and macro crack (left) (Banthia, 2012)

Quickly after placement, the evaporation of water in concrete start and the autogenous procedure of concrete hydration cause shrinkage strains. If controlled, this contraction could cause stresses more than those required to cause cracking. However, plastic shrinkage cracks stay as a serious concern, mainly in a large area like slabs, on thin surface repairs, shotcrete linings and patching (Banthia, 2012). When combined with post-crack bridging capability of fibers, fibers reduce crack widths and cracks, areas when concrete is restrained (Banthia, 1994) (Figure 7).

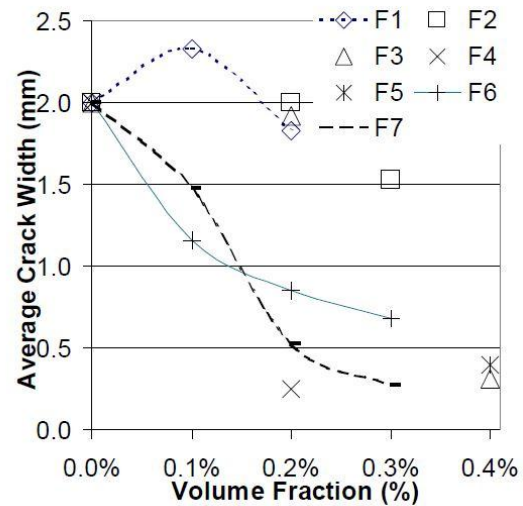
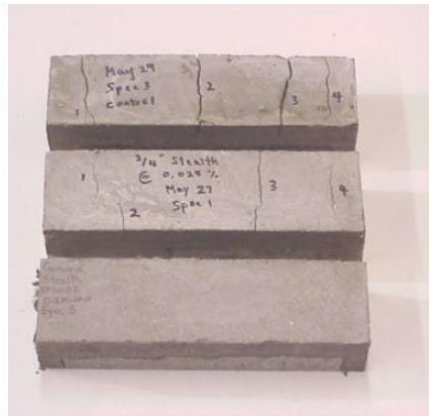
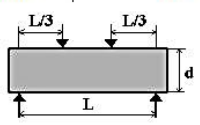
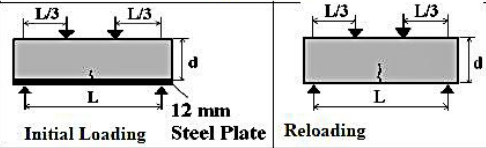
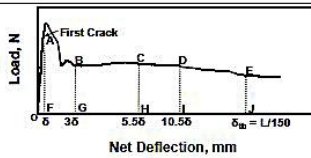
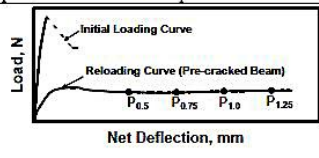


Figure 7: Crack of plastic shrinkage (left) and crack width (right) (Banthia, 2012)

2.3.2 Toughness Tests

Description of energy absorption or toughness of FRC over standardized testing is a difficult topic. There is not any specific agreement on measurement of FRC toughness (Banthia, & Trottier, 1995, Barr *et al.* 1996, Gopalaratman, 1992). There are three standards often used and two of these are ASTM (ASTM C 1609/C 1609M – 05 2006, ASTM C 1399-98 2004) and another one is JSCE (Japan Society for Civil Engineering). Table 2 shows these three methods and compares their analysis. Unfortunately, all treated toughness is different and just a little relationship can be seen between the parameters of toughness (Banthia, & Mindess, 2010). Toughness is the ability of a material to absorb and tolerant energy during loading and deformation which is measured by the area under the strain stress curves.

Table 2: Test method description (Banthia, 2012)

Standards	ASTM C 1609-08	JSCE SF-4	ASTM C 1399-98
Test Specimen			
Test Description	A beam specimen is quasi-statically loaded at its third-points to failure and the resulting load vs. net center point deflection is plotted for further analysis.		A stable narrow crack is first created in the specimen by applying a flexural load in series with a steel plate under controlled conditions. The plate is then removed, and the specimen is reloaded in flexure to obtain the post-crack load vs. net displacement curve.
Typical Curve			
Analysis	$P_{x,y}$ = Load at displacement y for a x mm section $f_{150,0.75}$ (MPa): Residual strength at $P_{150,0.75}$ $f_{150,3.0}$ (MPa): Residual strength at $P_{150,3.0}$ Toughness $_{150,3.0}$ (J): The energy to a net deflection of 1/150 of the span (3.0 mm for a 150 mm specimen)	Flexural Toughness (T_b) = Area OAEJ Flexural Toughness Factor (FT) $FT = \frac{T_b \times L}{\delta_n \times b d^2}$ $Re 2(\%) = \frac{FT}{MOR} \times 100$ MOR = Modulus of Rupture b = Breadth of the Beam d = Depth of the Beam	Average Residual Strength $ARS = ((P_{0.5} + P_{0.75} + P_{1.0} + P_{1.25}) / 4) \times L / b d^2$

A combination of steel fiber reinforcement and conventional reinforcement can improve the strain in tension and subsequently decrease crack width and spacing.

2.3.3 Cracking Behavior

Figure 8 illustrates the crack pattern. The steel fibers were observed to decrease the crack spacing. Figure 9 indicates the influence of the fiber aspect ratio and fiber content. It is worth to mention that the influence of fibers on the crack spacing rise by increasing the aspect ratio. It means that the more aspect ratio, the less crack spacing.

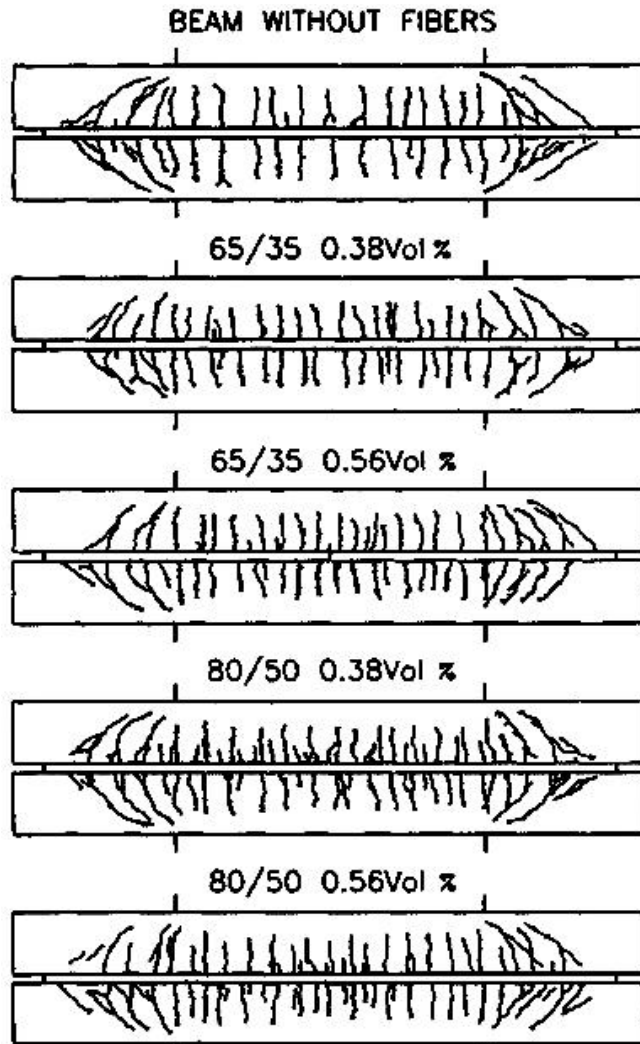


Figure 8: Crack pattern (Vandewalle, 2000)

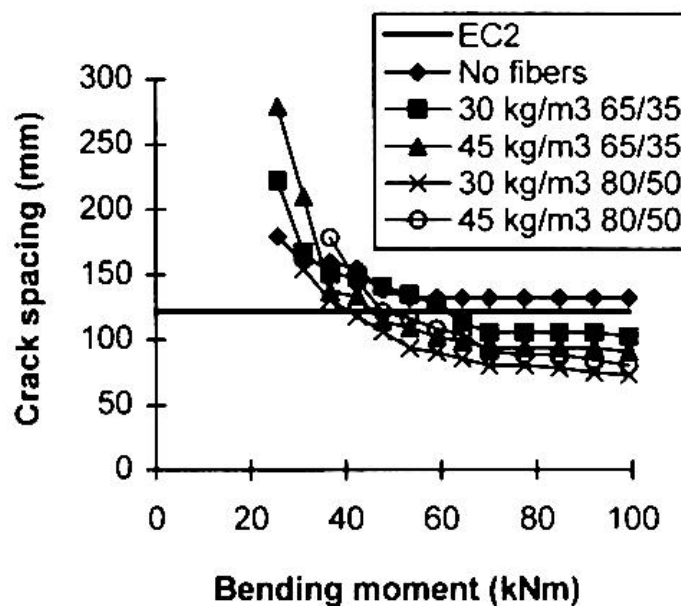


Figure 9: Average crack spacing (Vandewalle, 2000)

The formula to compute the mean crack width according to Eurocode 2 1991 owing to loading is:

$$W_{rm} = S_{rm} \times \epsilon_{sm} \text{ (mm)} \quad (1)$$

Where S_{rm} is the mean final crack spacing (mm), ϵ_{sm} is the average strain. For estimation the crack width, one needs to multiply W_m by 1.7 (Eurocode 2 1991). The mean final crack spacing can be computed by the equation 2 for the members that subjected to tension or flexure.

$$S_{rm} = \frac{-b \pm 50 + 0.25 \times k_1 \times k_2 \times \phi}{\rho} \text{ (mm)} \quad (2)$$

ϕ is bar size, k_1 is the coefficient of bond properties of bars, k_2 is the coefficient of strain distribution, ρ is an effective reinforcement ratio. The crack spacing is expected to be free of fiber content. Actually, two phenomena of steel fiber cause decrease of crack spacing in reality:

- Enhancement of the bond between concrete and rebar owing to the steel fibers,
- Post-cracking tensile strength of the steel fiber.

Based on Eurocode 2, ϵ_{sm} can be calculated by:

$$\epsilon_{sm} = \frac{\sigma_s}{E_s} \times 1 - \beta_1 \times \beta_2 \left(\frac{\sigma_{sr}}{\sigma_s} \right)^2 \quad (3)$$

Here, σ_s is tension stress (MPa) in reinforcement has been designed according to a cracked section as shown in Figure 10a, σ_{sr} is tension stress (MPa) in reinforcement and has been designed according to the first crack as shown in Figure 10a, β_1 is the coefficient of bond properties between bar and concrete, β_2 is the coefficient of the duration of the repeated loading or loading (Vandewalle, 2000).

Figure 10a and b show the cross-section without and with fiber respectively. Due to the less influence of fibers on pre cracking behavior, elastic behaviors in compression for calculating ϵ_{sm} in the cracked section has been assumed as shown in Figure 10b (Nemegeer *et al.* 1995).

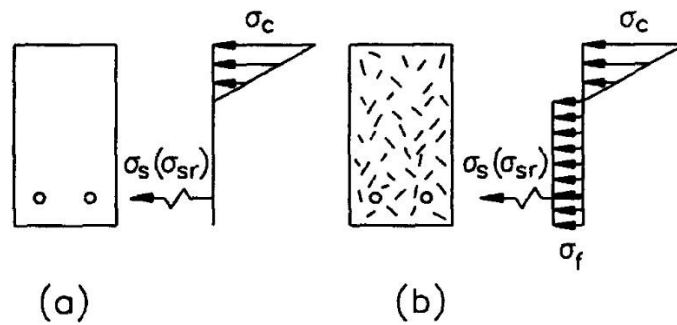


Figure 10: Distribution of stress in cracked section. (Vandewalle, 2000)

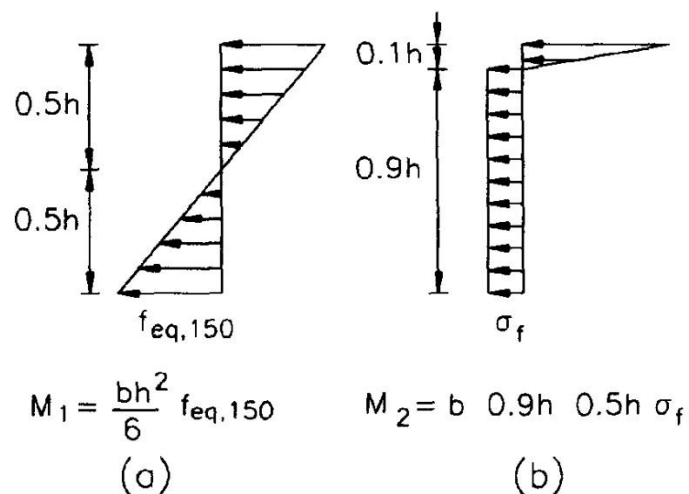


Figure 11: Tensile stress calculation (Vandewalle, 2000)

Figure 11 (a) shows a linear distribution of elastic stress, but actually, the distribution of stress is different in reality. To calculate a realistic stress in the cracked region, the next assumptions as given by Figure 11 (b):

- The crack height = 0.9 h;
- The tensile stress (σ_f) in the cracked region is constant.

There are some factors that can effect on the results, such as:

- Fiber dosage and type
- Fiber ratio to maximum aggregate size
- Mixing and batching
- Test size
- Laboratory experience and equipment

Supposing all other things stay constant (concrete strength, dosage, fiber type, mixing and batching etc.), the coefficient of variation in particular test method has been directly related to the area of cracks in concrete (Ross, 2001). If the fiber volume fraction is sufficiently high, this may result in an increase in the tensile strength of the matrix (Banthia, 2012).

When the beam reach to its tensile capacity and the conversion has occurred from micro-cracks to macro-cracks, fibers, according to their bonding characteristics and aspect ratio continue to confine the crack growth and crack opening by bridging through macro-cracks (Vikrant *et al.* 2012). The efficiency of all fiber reinforcement is dependent upon achievement of a uniform distribution of the fibers in the concrete, their interaction with the cement matrix, and the ability of the concrete to be successfully cast or sprayed (Brown, & Atkinson, 2012).

Fundamentally, each fiber requires being covered by a cement paste to do its duty sufficiently in the concrete. Moreover, adding of more fibers into concrete, has a negative result on workability. Hence, using super plasticizer can solve this problem without any harmful effect on other concrete properties. On the other hand, slump change because of the different kind of fiber content. The more surface area and

content of fiber, the more cement absorb to coat fibers. (Chen, & Liu, 2000, Mansur *et al.* 1986, Naaman, 2003, Campione, 2008, Campione, & Mangiavillano, 2008, Radtke *et al.* 2010).

2.5 Mix Design for SFRC

In order to improve the workability, production cost and decrease heat of hydration an appropriate replacement of cement with pozzolan would be beneficial (Gribniak *et al.* 2012).

2.5.1 Workability

The workability of SFRC is influenced by the parameters given below:

The main important issue that the workability of SFRC is involved with is to receive a suitable distribution of fibers in concrete.

- This difficulty is typically handled by slowly and continuously adding fibers into the mix.
- Adding water in terms of improving workability can decrease the flexural strength.

2.5.2 Test of Workability/Consistency

The some useful workability/consistency tests are:

- Slump test
- Inverted cone time
- Compacting factor test
- VeBe test (Figure 12-13)

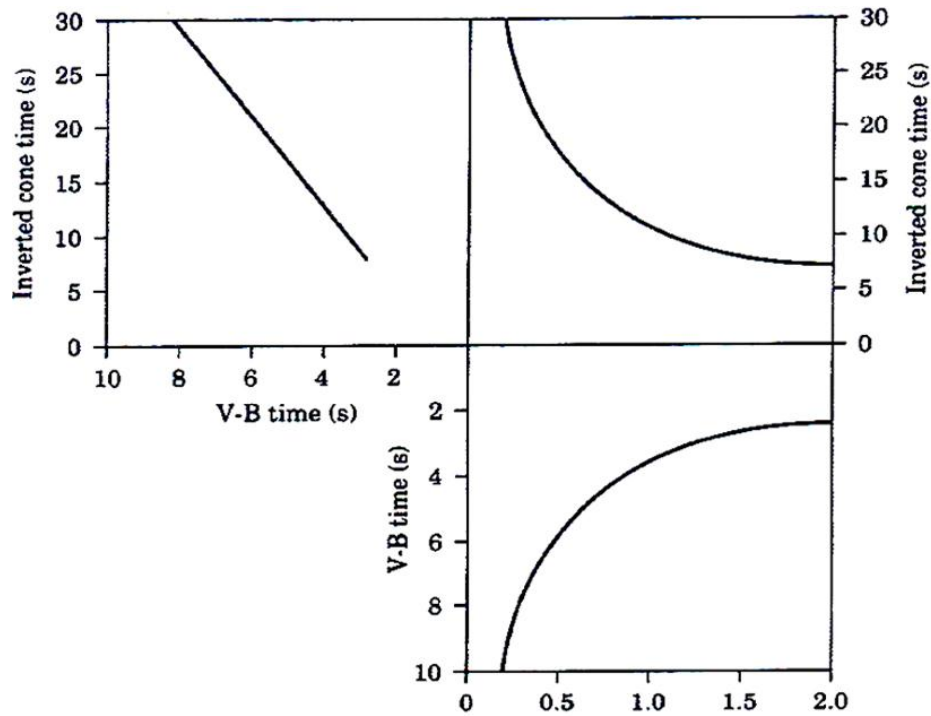


Figure 12: Relationship, between inverted cone time, VeBe time and slump (Nataraja, 2011)

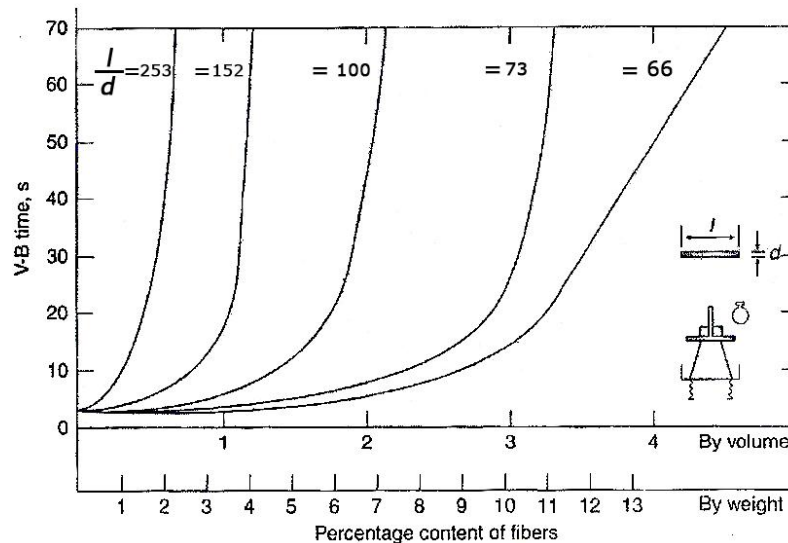


Figure 13: VeBe time vs fibers percentage (Nataraja, 2011)

Marini *et al.* (2008) have studied the performance of a fiber reinforcement concrete diaphragm while transferring vertical load to perimeter structure. They can determine that by increasing fiber content, the thickness of the elements could be reduced. Statistically, stirrups in a beam along fiber can increase shear strength significantly in comparison to plain concrete. Marini *et al.* (2008) reported that the FRC jacketing is

an effective method for FRC beam with stirrups for shear strengthening. In terms of replacing stirrups by fibers, he conducted that the failure of the beams without stirrups occur in a large side of beams suddenly, and the crack is wider than the ability of fibers to create bridges across it (Ruano *et al.* 2014).

This investigation tried to assess the shear ability of (High Performance Fiber Reinforced Concrete) HPFRC with a passive hybrid system and pre stressed longitudinal bars. Two beams have been tested with different pre-stressing level, three times. The pre stressing level, which effects on shear capacity was the key investigated parameter. The results indicated that the energy absorption and improvement of load carrying capacity have been increased by increasing the level of pre stress.

Figure 14 represents the average force vs mid-span deflection diagram which conducted that by increasing the level of pre stress, the capacity of load carrying have been increased without any significant effect on deflection at the maximum load (Soltanzadeh *et al.* 2013).

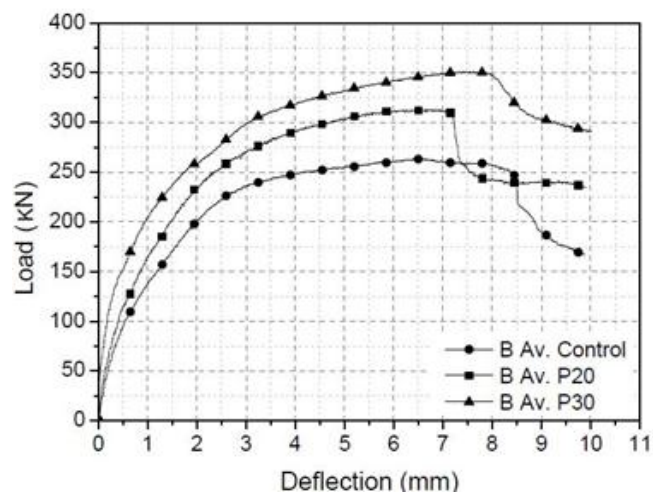


Figure 14: Average Load-Deflection at the mid-span (Soltanzadeh *et al.* 2013)

SCC contains 0.3 % fiber by volume, which has been used in pavement concrete. For decreasing segregation use of condensed silica fume is necessary. Adding a copolymer based super plasticizing was typically done at the ready-mix plant, and it was detected that slump flow increased from 20 to 30 mm. The copolymer type was tested as well and there has an influence on fibers segregation (Soltanzadeh, *et al.* 2013). Segregation is a challenge and the best mix which was used by Ding *et al.* (2011) is shown in Table 3.

Table 3: Concrete composition (dry materials) (Ding, 2012)

Concrete Composition	kg/m ³	l/m ³
Norcem Anlegg CEM I 52.5 N-LA (HSC)	255	82
Norcem Industri CEM I 42.5 RR (RPC)	91	29
Condensed silica fume from Elkem	26	12
Free water	212	212
Absorbed water	17	
Fine aggregate, 0-8 mm from Vang	850	
Fine crushed sand, 0-0.5 mm from Feiring	147	
Crushed aggregate, 8-16 mm	620	
Copolymer, Glenium 27, Degussa	6.7	
AEA Scanair 1:9	8.4	
Volume Bekeart RC65/60 steel fiber	66	8
Paste volume		340
Matriz		375
Matrix plus 5 % air		425
Nominal concrete density excluded fibers	2203	

Increasing the volume of matrix plus air is the main reason to use air entraining agent. For preventing of segregation and increase the flow of concrete, air bubbles

are helpful. Air bubble has less influence on cement paste, however, decrease the water content and cost (Hammer, & Johansen, 2008).

2.6 Previous Studies

2.6.1 SFRC Constitutive Concept in Compression

Fritih, *et al.* (2013) studied the influence of fibers through the local and global mechanical properties of the beams. According to the results fiber can improve the control of cracking. Fibers can't modify load bearing capacity, yielding and ductility. It just affects the distribution of cracks and kinetics. The stresses decrease in stirrups with the presence of fibers, but it doesn't mean that we are allowed to substitute fibers instead of stirrups. On the other hand, using fibers can reduce bar reinforcement ratio and makes the beam stiffer. They mention that for aggressive environments, stainless steel fiber should be used.

According to the research which was conducted by Banthia, & Trottier, 1994; Cucchiara *et al.* 2004; Edginton *et al.* 1978; Ezeldin, & Balaguru, 1989; Furlan, & Hanai, 1997; Khuntia, & Stojadinovic, 2001, transfer stress through a crack is the key role of fibers and therefore it can restrain the propagation and opening of cracks and increases the mechanical properties, mostly the post-cracking performance. Narayanan, & Darwish, 1987, Cucchiara *et al.* 2004 have observed that after flexural cracking the density of crack network have been increased. Oh, 1992 remarked that fibers in control of crack are better, and can reduce the cracks widths. Additionally, the fibers effect on stiffness, ultimate load and shear strength increases (Frosch, 2000; Mirsayah, & Banthia, 2002; Shin *et al.* 1994).

2.6.2 Direct Tensile Tests

In the direct analysis, structural response is based on specified model, but on the other hand, in inverse analysis intend to determine the parameters of the model according to the response of structures. For given experimental moment-curvature curve, a stress-strain relationship was defined from the equilibrium equations of the axial forces and the bending moments. To investigate the fibers influence on residual post-cracking strength by direct tensile tests, notched prismatic specimens ($100 \times 100 \times 200 \text{ mm}^3$) have been used. As can be seen in the Figure 15, for SCC, the diagrams illustrated brittle behavior and a sudden reduction in the residual strength with the rise of the crack opening after the ultimate load. By localizing the macro crack little energy needs to propagate cracks (Fritih, 2013).

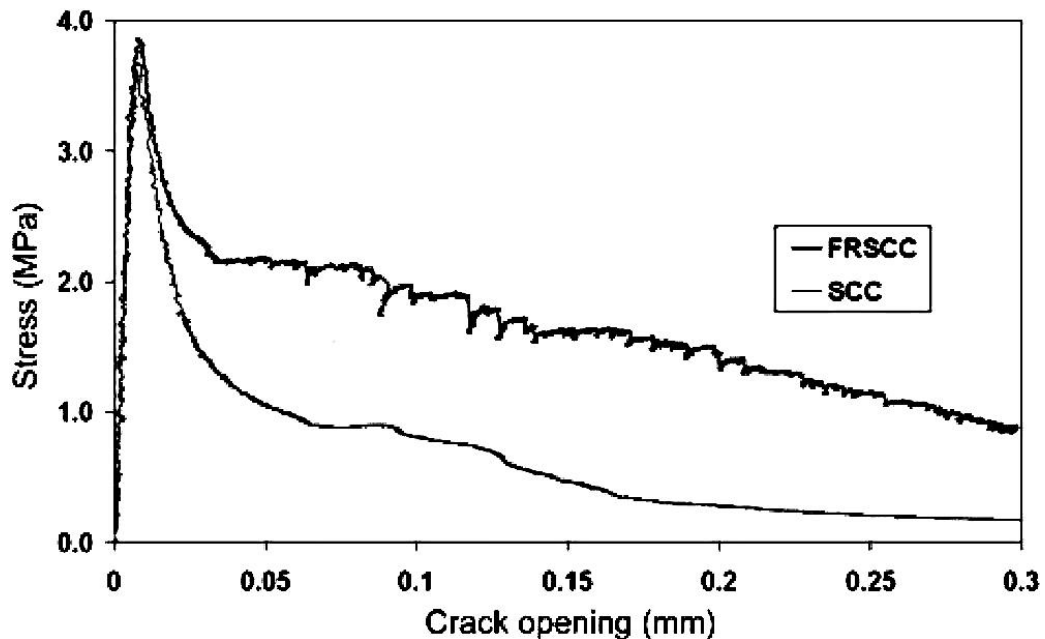


Figure 15: Crack opening versus residual post-peak strength crack opening in a direct tensile test on notched specimen (Fritih, 2013)

As can be seen in the Figure 15, the differences in FRSCC diagram just after the peak load, before that both diagrams are the same. According to the diagram, starting micro crack and propagation relates to just before the peak of stress. FESCC post-

peak behavior can be arranged as a three phase law. The first part relates to a stress reduction from peak to residual strength plateau. Fibers help to increase the residual strength and maintain crack opening where a residual strength is close to zero at SCC. The residual strength falling in softening materials during the growth of crack opening.

Post peak residual strength which is plateau placed in the second phase. This plateau is fundamentally influenced by fibers properties (bond with the matrix, modulus of elasticity) and fiber content. The fibers create a bridge in cracks and it cause stress concentration which leads to a plateau. It is short but on the other hand, the amplitude of the residual strength is high. The third part corresponds to the sample's failure. It is related to the continuous fracture of fibers. As said by Turatsinze *et al* 2005, the fibers can't resist against crack openings greater than 0.2 mm.

2.7 Crack Patterns

Figure 16 shows the crack pattern for FRSCC and SCC at regular load. Table 4 indicates a global combination of the cracking type of failure, including the length and number of cracks (the distance is between the two dangerous cracks), the normal spacing among consecutive cracks is the maximum crack opening width. In all samples, cracks initiate with flexural crack and situated in the middle of beam with maximum moment (the load value is from 10 kN to 15 kN). Others flexural cracks are in the high level of loading. The cracks which appeared near the support are for shear cracks by 35% to 50% of ultimate load and spread to the loading points. In the case of fiber concrete, the crack spacing is reduced, whereas the network of cracks, becomes denser than the beam without fibers. In fiber reinforcement beams the crack

propagation has a delay when compared to plain concrete in terms of height and opening.

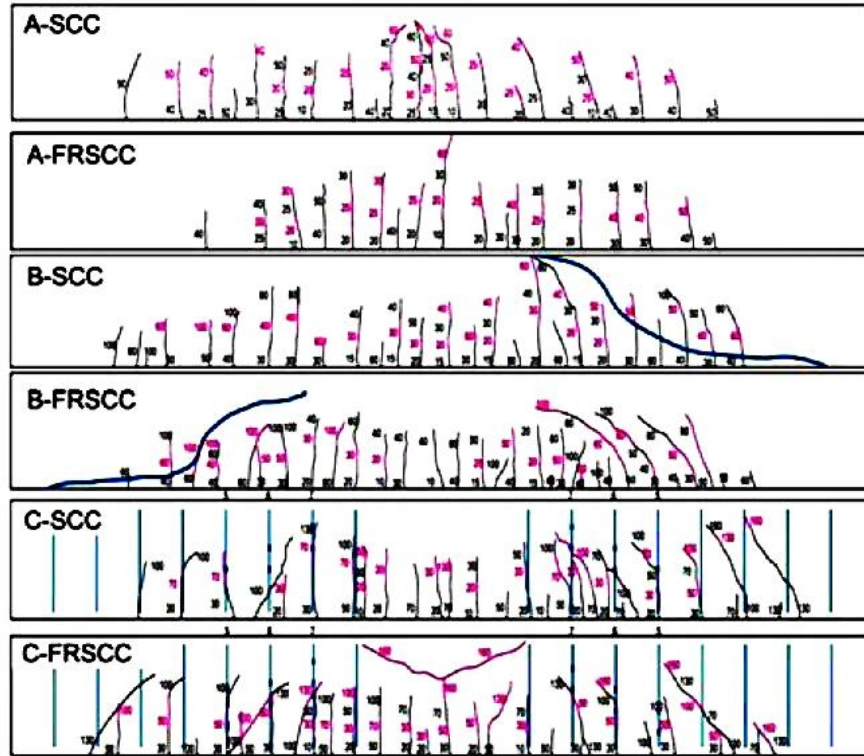


Figure 16: Crack pattern and loading levels on beams (Fritih *et al.* 2013)

Table 4: Effect of fiber reinforcement on cracking observed at the failure level

Beams	Number of cracks	Length of cracked Zone (cm)	W_{max} (μm)	W_{max} reduction (%)	Average crack spacing (cm)	Spacing reduction (%)
A-SCC	22	208	270	33.3	10.5	7.6
A-FRSCC	19	175	180		9.7	
B-SCC	26	220	213	10.3	8.8	13.6
B-FRSCC	31	228	191		7.6	
C-SCC	28	242	361	16.9	9	13.3
C-FRSCC	29	220	300		7.8	

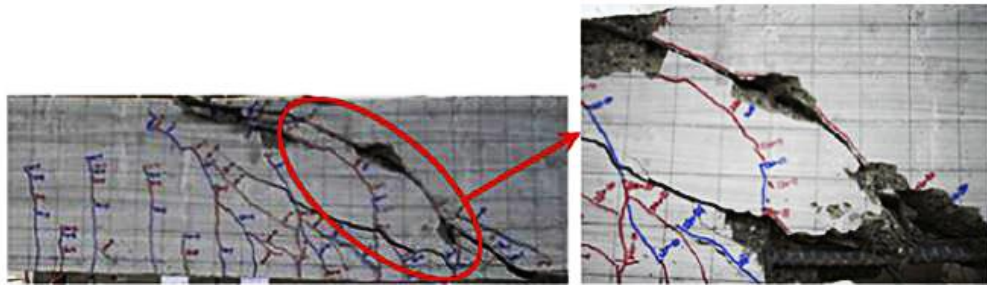
Therefore, the tensile strength seems to be enhanced due to the influence of fibers between two flexural cracks.

Before starting the first cracks, the FRSCC beams and plain beam (SCC) had similar behavior according to load against deflection response. At this step, the stiffness development did not rely on the existence of fibers. By initiating the first crack, all specimens illustrated a nonlinear response. In the stabilized cracking stage under service load, stiffness have got a small increase in the Figure 16 “A” beam (A-FRSCC) only. SCC and FRSCC have similar behavior in the bending stiffness. Load bearing capacity, ductility and yielding were not significantly improved by the fibers. Generally, fibers improve tension stiffening and stress transfer over the cracks and can confine crack opening.

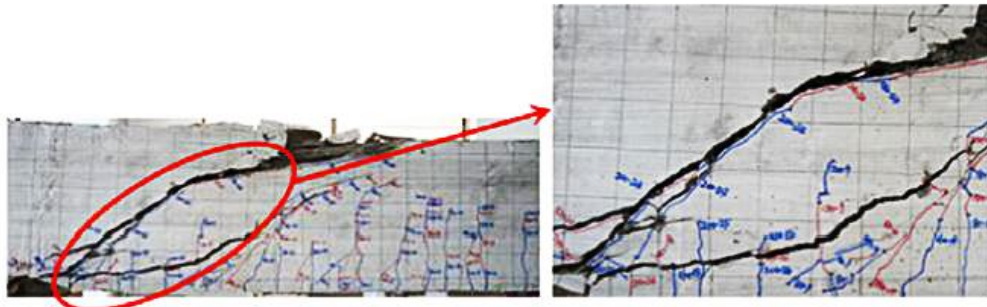
Figure 17 (a) illustrates the failure pattern of SCC beam which doesn't have fibers. By developing and widening of diagonal cracks, the resistance of beam decreases abruptly. Near the longitudinal reinforcement the dowel failure and concrete spalling action can be observed. The following explanations have been taken by comparing two beams (SCC and FRSCC) from Figure 17 (a) and (b).

- The distributed fibers can absorb some part of shear force.
- The three-dimensional fibers can resist the diagonal cracks; thus, a great residual compressive strength in uncracked zone can be well-maintained.
- Fiber bridging increase the resistance of aggregate interlocking significantly. Fibers that are erected to the diagonal cracks, can increase the shear strength visibly as shown in Figure 17(b).

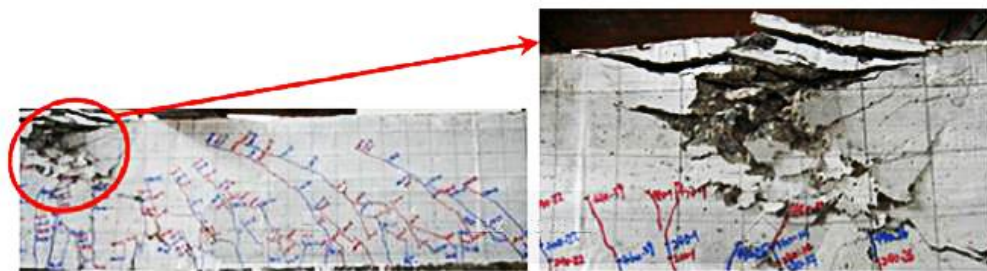
- The spalling and dowel failure around the bending steel prevent significantly. In this case, the fibers that are in the same direction of longitudinal bars have more sufficient effect compared to other orientations.
- The fibers decrease the strain in stirrups and longitudinal steel at ultimate stress.
- The tension capacity increases by steel fibers and somewhat absorbs tensile stress (Ding *et al.* 2011).



(a) SFSCCB0-150 with failure of dowel action, spalling, and strong brittle diagonal cracking.



(b) SFSCCB25-150 with less brittle diagonal failure.



(c) SFSCCB50-150 with ductile flexural failure.

Figure 17: Failure and crack pattern of beams with 0.22% stirrup ratio (Ding *et al.* 2012)

Vecchio, & Collins, 1986 used to calculate the tensile stress effect on crack concrete.

They tried to obtain by detecting the response of a lot of reinforced concrete

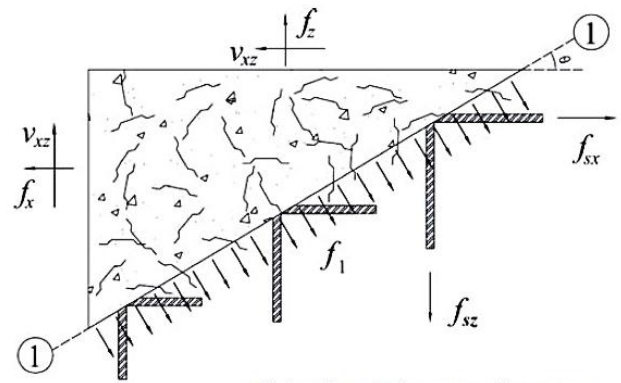
elements that subjected to shear load with axial stress together or pure shear load. It is remarkable to note that the FRC is more appropriate than the concrete without fibers, owing to its stress strain relationship that is flatter in the tension and in the post peak level of compression in comparison with plain concrete (Collins, & Mitchell, 1991).

Figure 17 (a) and Eq 4 have compared the actual local stresses by diagram of fiber reinforcement element with calculated average stress. Through the average shear stress by Eq 4 equal zero, therefore it could be local shear stress on Eq 5.

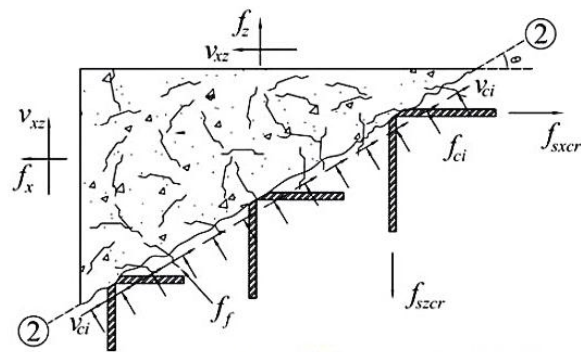
$$\rho_{sz}f_{sz} \cos \theta + f_1 \cos \theta = \rho_{sz}f_{szcr} \cos \theta - f_{ci} \cos \theta + v_{ci} \sin \theta + v_f \sin \theta + \sigma_f \cos \theta \quad (4)$$

By increasing the loads, stirrups strain (ϵ_z) will surpass yield strain of transverse steel. At this moment, both f_{szcr} and f_{sz} will equal to the stirrups yield stress, subsequently we can get:

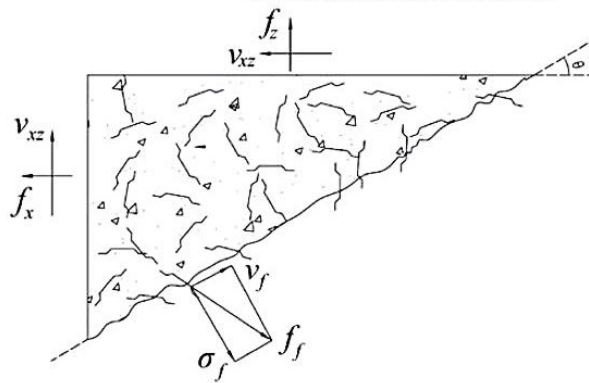
$$f_1 = (v_{ci} + v_f) \tan \theta + \sigma_f \quad (5)$$



Calculated Average Stresses



Local Stresses at a Crack



Stress component of a single fibre transferred perpendicular to crack and parallel to crack

Figure 18: Comparison of local stresses at a crack with calculated average stresses of SFRC and stress state of a single fiber (Ding *et al.* 2012)

2.8 Toughness

$(D_8^f; f_{eq:8}^f)$ are two parameters of toughness which are presented to assess the capacity of energy absorption and the capacity of the residual load bearing of beams for this deflection $\delta_8 = \delta_{cr} + 8$ mm.

D_8 is the area below the load–deflection curve, which is the entire energy absorbed until the δ_8 (certain deflection). By using below equation, one can calculate the equivalent strength:

$$f_{eq8}^f = \frac{D_{8ls}^f}{6b_w d^2 v} \quad (6)$$

The beams with stirrups exhibited low toughness. By using both fibers and stirrups indicated a progressive hybrid effect to improve the toughness and post-peak behavior (Figures 19 and 20) (Ding *et al.* 2012).

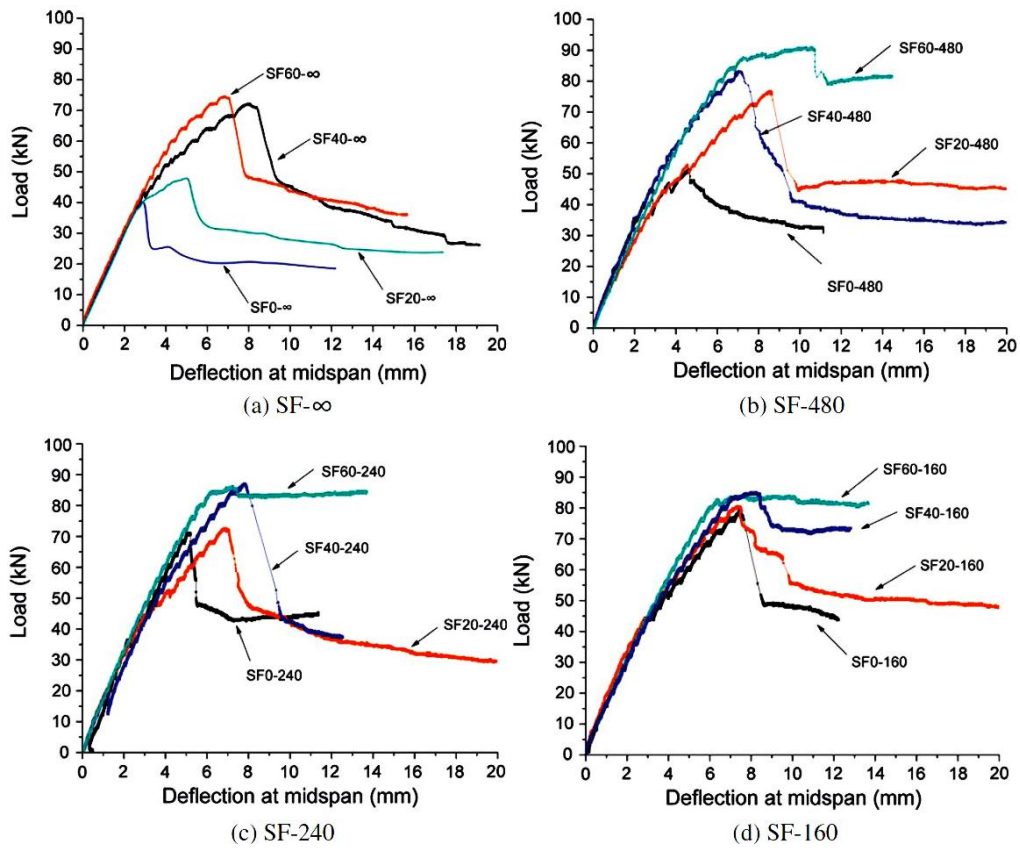


Figure 19: Load vs deflection responses in beams with diverse stirrup ratios (Ding *et al.* 2012)

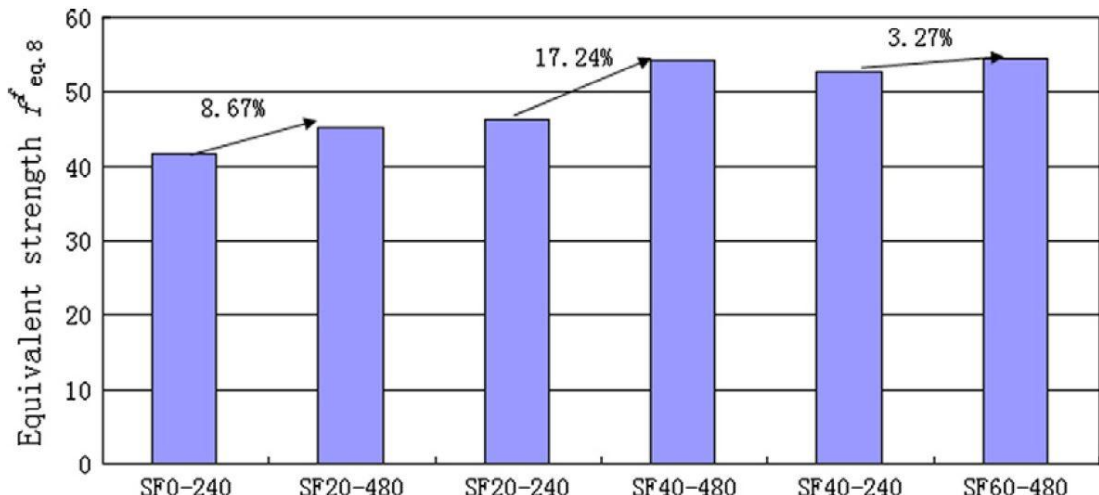


Figure 20: Increase of toughness factor for beams with various reinforcements (Ding *et al.* 2012)

Chapter 3

METHODOLOGY

3.1 Introduction

This study has focused on two classes of concrete C20 and C40. The effect of steel fiber quantity of fiber reinforcement self-compacting concrete slabs is assessed. In each class of slab, four different amount of fibers have been tested namely 0%, 1%, 1.5% and 2%. For each type, two slabs were constructed.

3.2 Experimental Module

3.2.1 Specimens Provision

In this study the test requirements are 4 shafts and an IPE400. Two of the shafts beneath the slab were used as support and the next two shafts were placed under the IPE400.

Due to the limitation for applying two point load separately, 100 kN load should be divided into two 50 kN by using I shape profile as can be seen in the Figure 21. For this purpose, ANSYS software was used to model the required dimensions as shown in Figure 22. By definition the slab size and load, it can define the appropriate size of plats, shafts and IPE. Figure 21 shows the stress in the different part of slab, IPE and shafts. According to that, the IPE and shat should be remind without any deformation.

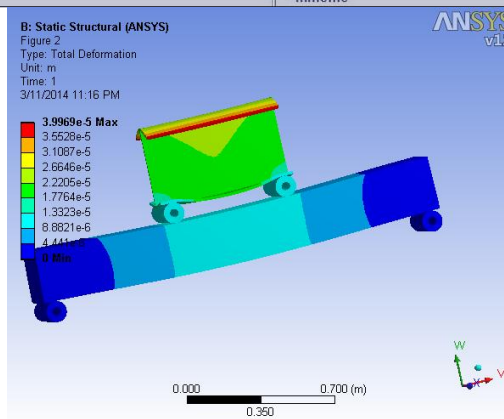
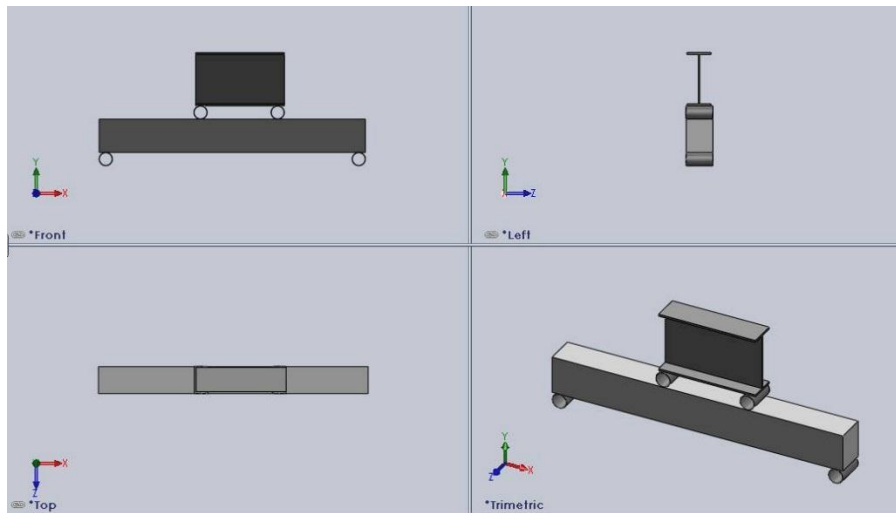


Figure 21: IPE and slab deformation

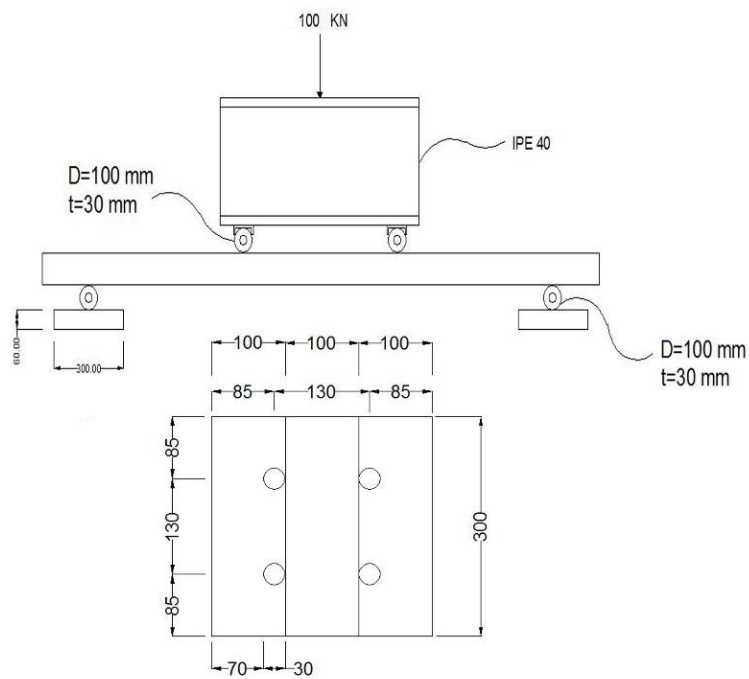


Figure 22: Dimensions of plate, shaft and IPE

Table 5: Requirement tools and dimension

	Number	Length	Width	Diameter	Thickness	Kind	Available
Plate	2	300	300	-	60	-	No
Shaft	4	300	-	100	30	-	No
Channel						-	
(U shape)	2	300	-	-	-		No
IPE	1	1000	-	-	-	IPE 400	No
Bolt	8	150	-	30	-	HV 10 9	Yes
Nut	8	-	-	-	-	HV 10	Yes
Bar	40	2500	-	ϕ12	-	-	No
Wood							
Of	28	3000	100	-	-	-	No
Formwork							

3.2.2 Evaluation of the Load Required

Two different slabs (SCC and FRSCC) have got different load capacities. The SCC slab that is called plain slab can tolerate the load which was calculated in Figure 23:

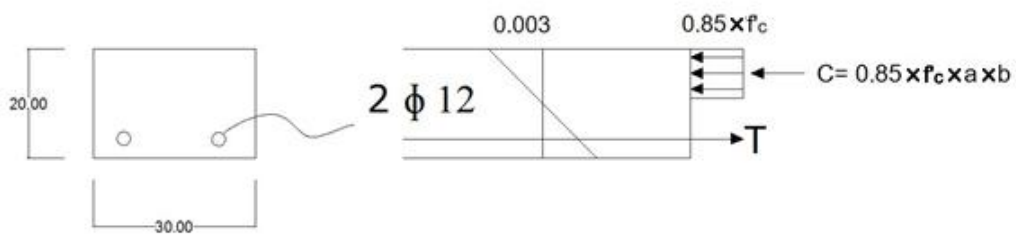


Figure 23: Load capacity of SCC

$$T = A_s \times F_y = \left(\frac{2 \times \pi \times 12^2}{4} \right) \times 420 = 94953.6 \text{ N} \quad (7)$$

$$a = \left(\frac{T}{0.85 \times 20 \times 300} \right) = 18.61 \quad (8)$$

$$M_r = A_s \times F_y \times \left(\frac{d-a}{2} \right) = 15.25 \text{ kN.m} \quad (9)$$

$$P = \left(\frac{M_r}{L}\right) = 22.7 \text{ kN} \quad (10)$$

3.2.3 Concrete and Mix Design

The selected strengths of concrete in this study were C20 and C40 MPa for standard cube specimen (150×150×150 mm). For each mix design, three samples were tested at 7-days and 28-days.

The Portland 32.5 cement class was used. The aggregates chosen were 10, 14 and 20 mm, and the fine aggregate was 5 mm. For reaching the best result of super plasticizer, tried to test more than 10 different percentages of SP. At the end, 1% for C20 and 2% for C40 was selected. Each slab contains two bars (12φ) with 90 degree hook end (Figure 24).

For self-compacting fiber reinforced concrete some test, such as, slump, J-ring, L-box, V-funnel and T50 should be done. During this research, one type of fiber was used with length over diameter “60/30” as shown in Table 6.

Table 6: Steel fibers characteristics

Fibers Types	Effective Length (mm)	Diameter (mm)	Tensile Strength (MPa)	Density (kg/m ³)	Aspect Ratio (l/d)
60/30	30	0.5	1345	7850	60



Figure 24: Formwork construction and bars

3.3 Sieve Analysis

This test is needed to determine the percentage of materials for coarse and fine aggregate (ASTM C 136, 2006). In this research, four different aggregates sizes have been used namely 5, 10, 14 and 20 mm based on ASTM C 136, 2006 (Tables 7-11):



Figure 25: Sieve analysis

Table 7: Sieve analysis for 20mm D_{max} of aggregate

BS sieve size (mm)	Weight retained (gr)	Percentage retained (%)	Cumulative percentage retained (%)	Cumulative percentage passing (%)
28	19	1	1	99
20	546	18	19	81
14	1573	52	71	29
10	641	21	93	7
6.3	139	5	97	3
5	15	1	98	2
pan	65	2	100	0
Total Weight	2998			

Table 8: Sieve analysis for 14 mm D_{max} of aggregate

BS sieve size (mm)	Weight retained (gr)	Percentage retained (%)	Cumulative percentage retained (%)	Cumulative percentage passing (%)
28	0	0	0	100
20	0	0	0	100
14	154	5	5	95
10	1516	51	56	44
6.3	1319	44	100	0
5	2	0	100	0
pan	4	0	100	0
Total Weight	2995			

Table 9: Sieve analysis for 10 mm of aggregate

BS sieve size (mm)	Weight retained (gr)	Percentage retained (%)	Cumulative percentage retained (%)	Cumulative percentage passing (%)
28	0	0	0	100
20	0	0	0	100
14	0	0	0	100
10	2	0	0	100
6.3	1474	49	49	51
5	797	27	76	24
pan	723	24	100	0
Total Weight	2996			

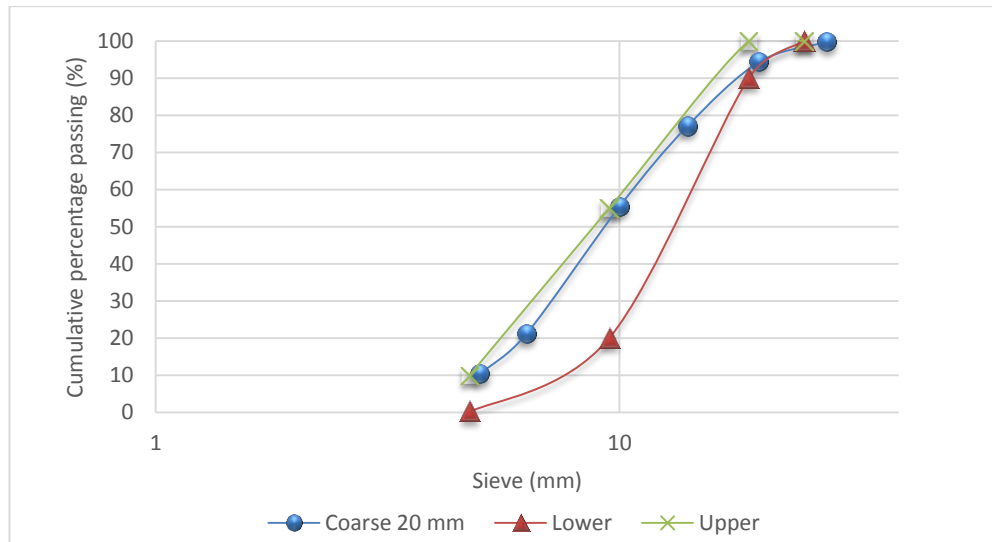


Figure 26: Sieve analysis for coarse aggregate

Table 10: Sieve analysis for 5 mm of fine aggregate

BS sieve size (mm)	Weight retained (gr)	Percentage retained (%)	Cumulative percentage retained (%)	Cumulative percentage passing (%)
4.75	0	0	0	100
2.38	235	12	12	88
2	232	12	23	77
1.19	381	19	42	58
0.841	200	10	52	48
0.595	226	11	64	36
0.297	255	13	77	23
0.177	102	5	82	18
0.149	62	3	85	15
0.074	129	6	91	9
pan	176	9	100	0
Total Weight	1998			

Table 11: Sieve analysis for 5 mm of aggregate

size	pass-lower	size	pass-upper
25	100	25	100
19	90	19	100
9.5	20	9.5	55
4.75	0.1	4.75	10

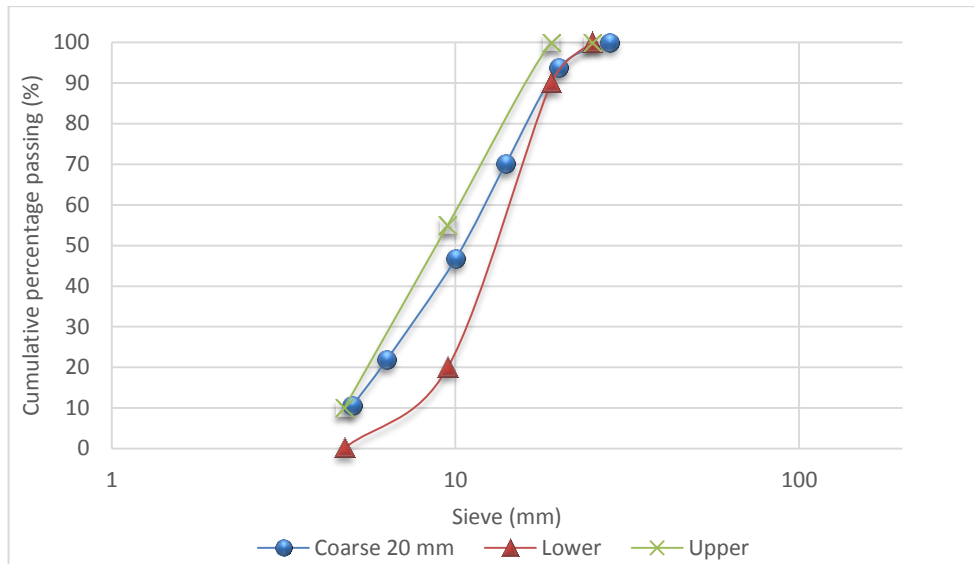


Figure 27: Sieve analysis graph fine aggregate

3.4 Compressive Strength Test

To find out the optimum percentage of super plasticizer, concretes containing 0.30, 0.5, 0.80, 1, 1.5, 2.5 and 3 percent admixture were cast. For each percentage and each class of concrete, 3 cubes were used in the following mix-design (Table 12) Eren, & Alyousif :

Table 12: Mix design for C20 Concrete

Mix	W/C Ratio	Cement	Water	Fine aggregate (gr)	Coarse aggregate (gr)		
				T ₅	T ₂₀	T ₁₄	T ₁₀
SCC (control)	0.5	4808	2404	14139	2289	2289	3052

Table 13: Mix design for C40 Concrete

Mix	W/C Ratio	Cement	Water	Fine aggregate (gr)	Coarse aggregate (gr)		
				T ₅	T ₂₀	T ₁₄	T ₁₀
SCC (control)	0.66	4808	3189	14139	2289	2289	3052

By decreasing the water to cement ratio from 0.66 to 0.5 the C40 concrete was reached. The mix started by adding coarse aggregate, fine aggregate and cement. After mixing dry materials in appropriate time (1 minute), water was added in two parts. The first part was used without SP and the second part water with super plasticizer was added. Then fibers were added slowly to avoid segregation. Table 14 shows the compressive strength test results of the cubes (150×150×150 mm) on the 7-day and 28-day for C20 and C40.

Table 14: Compressive strength test results for cube samples of C20

SP %	0	0.3	0.5	0.8	1	1.5	2.5	3
7-day	13.51	15.7	16.3	16.6	17.9	16.5	18.6	16.3
28-day	18.55	22.2	24.5	24.65	26.65	23.3	21.9	22.1

Table 15: Compressive strength test results for cube samples of C40

SP %	1	2
7-day	32.1	32.33
28-day	43.55	40.73

3.5 Testing Fresh SCC

3.5.1 Slump Flow and T50 Test

The slump test is intended to investigate the SCC filling ability. It considers two parameters: flow time T50 and flow spread. T50 indicates the rate of deformation in a specific distance and slump shows unrestricted deformability (Figure 28). The T50 test is the period when the cone leaves the base plate and concrete touches the circle (its diameter 500 mm). T50 is expressed in seconds. The slump flow spread S is the average of diameters d_{max} and d_{perp} , as shown in Equation (11). S is expressed in mm.

$$S = \frac{(d_{max} + d_{perp})}{2} \quad (11)$$



Figure 28: Slump and T50 tests

3.5.2 L-Box Test

The L-box test investigates the passing ability and it measures the height of fresh concrete after passing over the specified openings of three smooth bars (12 mm diameter) and flowing in a defined distance. During this test, the blocking or passing behavior of fresh concrete can be assessed.

3.5.2.1 Test Procedure

The vertical part fill by 12.7 liters of FRSCC and after resting concrete for 1 minute, let the concrete flow by opening the sliding gate Figure 29. After stopping the concrete, measure the height of concrete in two part starting point h_1 and ending point h_2 of the horizontal box ACI 237R-07.

$$\text{L-box blocking ratio} = \frac{h_2}{h_1} \quad (12)$$



Figure 29: L-box test

3.5.3 J-Ring Test

This test investigates both the passing and filling ability of FRSCC. The J-ring test considers three parameters: flow time T50J, flow spread and blocking. The J-ring flow test shows the restricted deformability of fresh concrete because of blocking effect of ring (reinforcement bars) and the T50J shows the rate of deformation in a defined distance (500 mm) ACI 237R-07.

3.5.3.1 Test Procedure

This test is exactly like slump test just add a ring around the cone of slump. After filling the cone and placing the ring, the cone leaves and the time of the first touch of concrete to the circle (500 mm) should be recorded (T50J) ACI 237R-07. After stopping the concrete the longest diameter and the perpendicular diameter measured Figure 30. The J-ring spread S_J is as shown below:

$$S_J = \frac{(d_{max} + d_{perp})}{2} \quad (13)$$



Figure 30: J-ring test

3.5.4 V-Funnel Test

This test indicates the filling ability of concrete and its time some degree connected to

plastic viscosity as shown in Figure 31.



Figure 31: V funnel equipment

3.5.4.1 Test Procedure

During the V-funnel test, fresh concrete should be filled by opening the gate and timer should be started until the first light is seen as shown in Figure 32.



Figure 32: V funnel test

3.4.1 Casting and Curing

According to ASTM C39, 2014 the cubes were tested on 7 and 28 days. Three samples for 7-days and three samples have broken at 28-days (ACI 301, 1999). The result of 7-days are not used for acceptance but there are some experimental approaches says that it is about 0.75 percent of 28-days, on the other hand ACI does not accept this format.

Cylindrical specimen is suggested by the ASTM C39/C39M code, but according to some researchers cube samples has about 80 to 90 percent value of the cylinder sample (Shetty, 2005). The dimensions of the slab which was used in this research is 200×300×2200 mm with two bars ϕ 12 and 90 degree hooked-end and 20 mm was the cover of reinforcement according to ACI318-11 as shown in Figure 33.



Figure 33: Slab formwork and steel bars

Super plasticizer has been used for increasing the workability, subsequently, it doesn't need any vibration and it was added according to the weight of cement. The first two slabs in each class of concrete belong to plain concrete without any steel fibers. For the

rest of samples, fibers were added according to the concrete volume percentage (FRSCC) as shown in Figure 34. After casting the slabs and cubes, the water curing started from their surfaces. Until 28-days cubes were kept curing room.



Figure 34: Slab filled with SCC

3.5 Flexural Test Setup

3.5.1 Test Apparatus

The slab has been designed according to the flexural and for this reason shouldn't fail by shear. For preventing the shear failure and increasing moment in the middle of the slab, the point load located at 500 mm at the middle of slab and 4 strain sensors were placed at the top and bottom of each slab and also a transducer was placed at the bottom center of it (Figure 35).



Figure 35: Test apparatus for flexural strength

Chapter 4

ANALYSIS, RESULTS AND DISCUSSIONS

In this chapter, the results of concrete test, load-deflection and moment-curvature was discussed by focusing on the class of concrete, fiber percentage and behavior of the slabs.

4.1 Results of T₅₀, Slump, L-box, V-Funnel and J-Ring

The results of self-compacting concrete test were revealed in the Table 16. In both kinds of concrete, fibers decrease the concrete passing. As can be seen in the Table 16, the time of T₅₀, V-Funnel and J-Ring increased by increasing the percentage of fibers and L-Box height decrease in the lower level.

Table 16: Workability test results of Self-Compacting Concrete

	Fiber %	T ₅₀ (sec)	Slump (cm)	L- Box (cm)	V- Funnel (sec)	J-Ring		
						T _{50J} (sec)	S _J (cm)	B _J (cm)
C 20 (1%SP)	0	0.63	68.5	0.9	7.35	0.87	64.5	2
	1	1	61.5	1	12.94	2.12	68.5	2.55
	1.5	1.93	68.5	0.2	18.37	2.47	59	3.725
	2	1.56	71	0.09	23.45	1.73	63.5	7.4
C 40 (2%SP)	0	0.41	92	0.29	8.95	0.45	90	8.75
	1	2.01	61.5	0.22	1.00.59	0.68	69.5	6
	1.5	3.5	55	0	51.31	3.5	64	2.5
	2	2.48	49.5	0	48.78	2.6	58	3.75

4.2 Compressive Strength Test Results of Cubes

For each slab three specimens (cube of 150 mm size) have been taken for compressive strength test. Results were shown in the following Table 17:

Table 17: Compressive strength results of cubes (MPa)

Fiber	7-days				28-days			
	0%	1%	1.50%	2%	0%	1%	1.50%	2%
C20	17.9	17.56	20.56	19.3	26.65	30.46	26.46	27.45
C40	32.33	31.67	30.13	31.7	40.66	42.27	41.3	42.77

4.3 Experimental Results of Flexural Test

4.3.1 TDS Setup

All slabs were loaded by TDS-303 machine in the middle, with distance of 500 mm for decreasing shear collapse as can be seen in Figure 36. A 10 mm transducer was used for measuring displacement exactly placed at the bottom middle of the slabs as shown in Figure 37. The data logger has 8 channels (3 channels for displacement, one channel for vertical load and 4 channels for strain sensor). In addition, 4 sensors (2 at the top and 2 at the bottom) were used for evaluating strain. The sensors coefficient needed to be calculated by the following formula:

$$k_0 = \frac{R}{R + \frac{r \times L}{2}} \times k = \frac{120}{120 + \frac{0.44 \times 2}{2}} \times 2.12 = 2.11$$

(14)

r = total resistance of load wires

L = length of load wires (m)

K = gauge factor

K₀ = Corrected gauge factor

R = gauge resistance

$$C_s = \frac{2.00}{k_0} = 0.95 \quad (15)$$

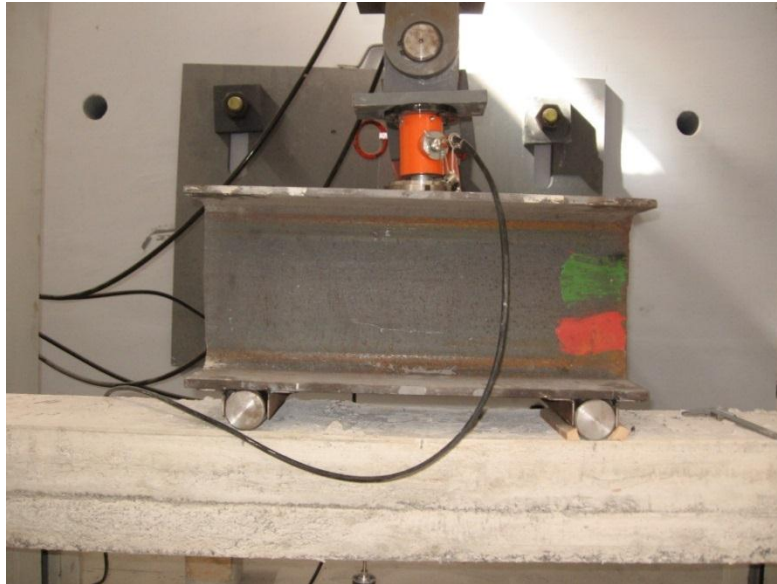


Figure 36: Test apparatus (load cell and IPE 400)



Figure 37: Test apparatus (load cell, IPE400 and transducer)

4.3.2 Slab with Different Percentage of Fibers for C40 Concrete

4.3.2.1 Mixture of 2% Super Plasticizer for - 0% Fibers

In this study, four slabs without fibers in two classes of concrete were tested. For each mix design which varied in percentage of fiber and compressive strength, the vertical load was applied and load-displacement and moment-curvature was taken. Below diagram illustrated load-displacement for the slabs with 2% super plasticizer and 0% fiber as shown in Figure 38.

By increasing load, the slab had a linear behavior before appearing the first crack and continue until failure. The first crack appeared at the same place on the load due to maximum shear and moment. Then the cracks appeared between two points of applied load which shows flexural cracks (Figure 38-39). By increasing the load, the slabs resistance was changed and goes into plastic mode until failure. During this mode the neutral axis went up because of the concrete at the bottom was yielded.

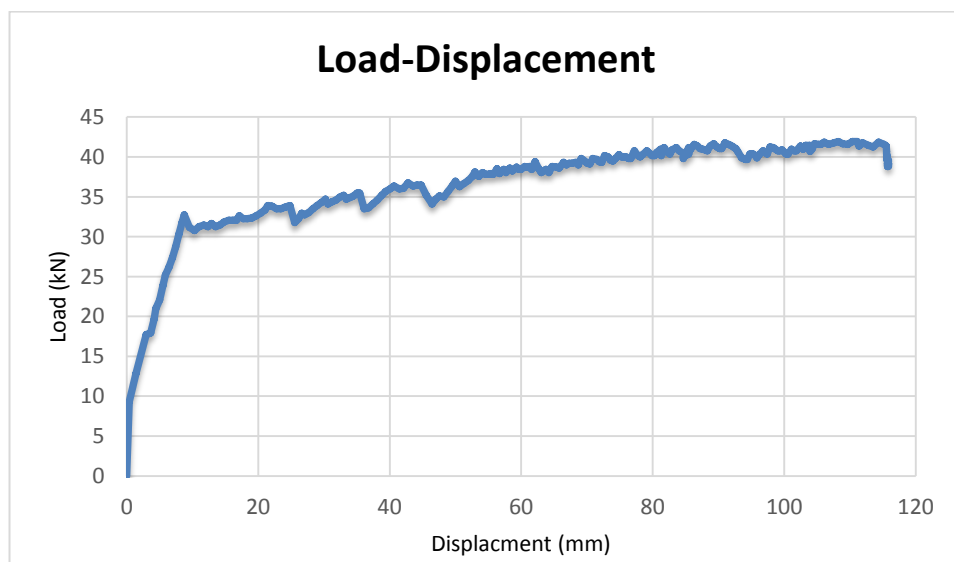


Figure 38: Load-Displacement diagram for C40 concrete (2%SP-0%Fiber)



Figure 39: Crack pattern for concrete C40 (2%SP-0%Fiber)

Figure 40 shows moment-curvature characteristic of 2% SP and 0% fiber. According to the diagrams, three significant zones are illustrated as elastic, crack and failure zone. In the first area, slabs had elastic behavior and by increasing the load this behavior changed to inelastic and tensile stress goes beyond the slab cracking stress. The cracks appear due to degradation in the flexural stiffness of the slab. At the end of the diagrams, loads were more than slab capacity and led to failure. In the middle area of the diagram, the fibers helped the bars to make a bridge for increasing the tensile stress.

At the end of diagram which showed post cracking behavior, bars started to yield and the tensile and compressive strength of slab decrease until collapsed. Normally, in the flexural behavior investigation, tensile stress of concrete was neglected because in the crack section, tensile forces could not transfer. On the other hand, in the presence of fibers the crack section could transfer tensile forces by bridging the cracks.

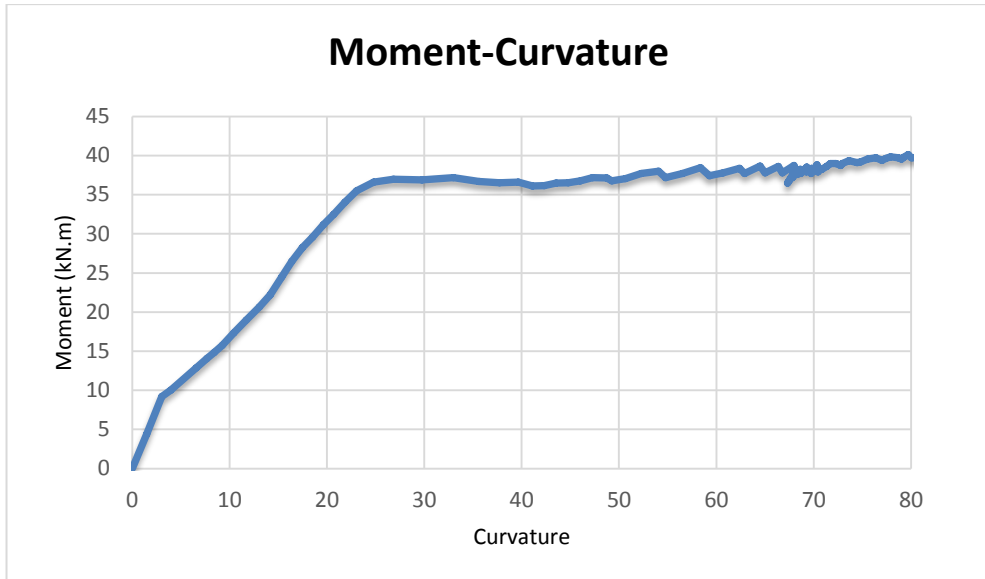


Figure 40: Moment-Curvature diagram for C40 concrete (2%SP - 0%Fiber)

4.3.2.2 Mixture of 2% Super Plasticizer for - 1% Fibers

Figure 41 indicated load displacement of 2%SP and 1%Fiber. It is clear that the amount of absorption of energy increased by increasing the percentage of fiber. The fiber's effect was revealed at the crack propagation. Figure 41 shows the effect of fiber to increase the tension strength by bridging through cracks.

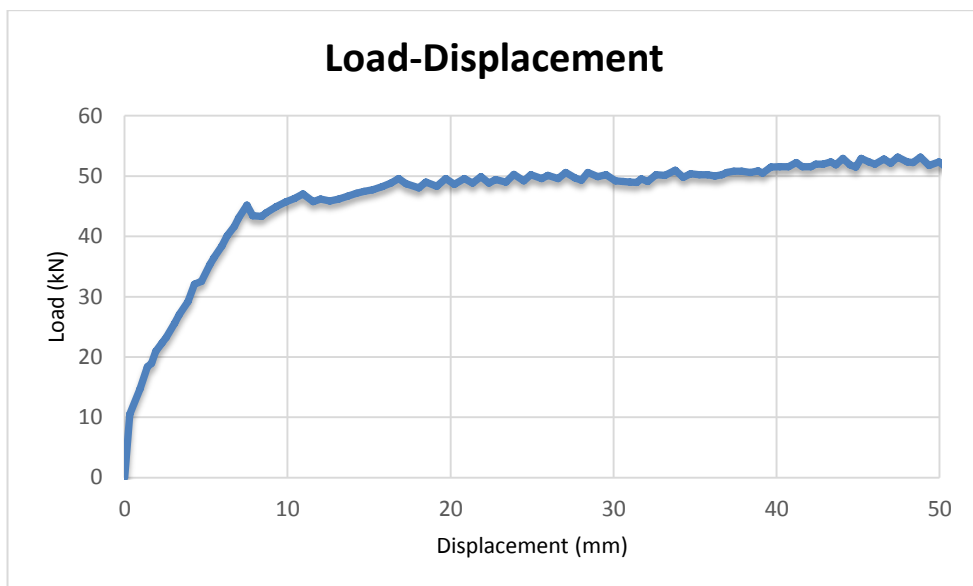


Figure 41: Load-Displacement diagram for C40 concrete (2%SP - 1%Fiber)



Figure 42: Crack section (2%SP - 1%Fiber)

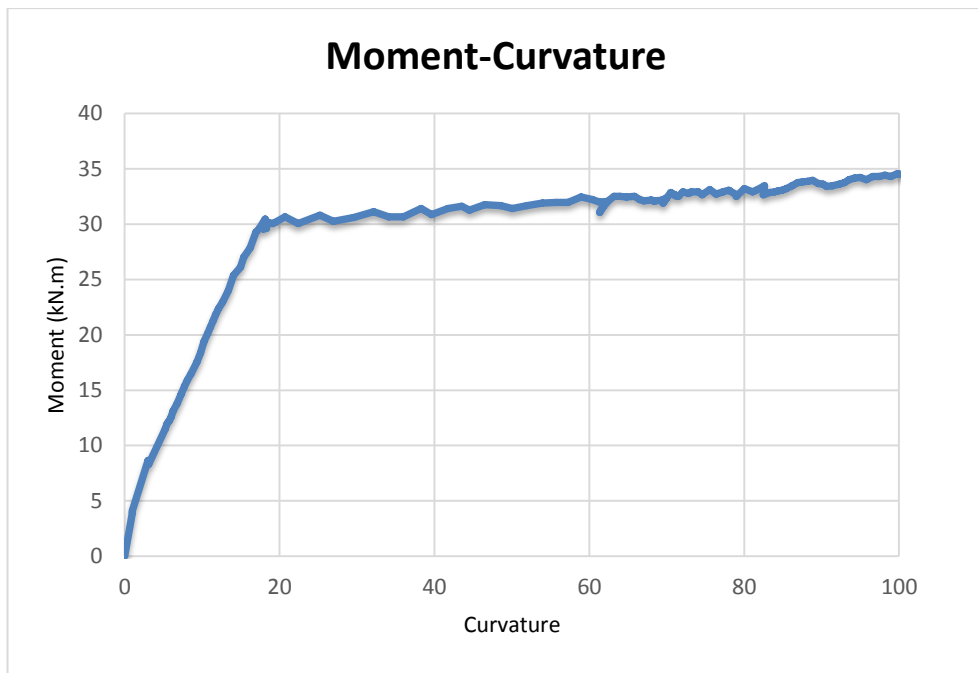


Figure 43: Load-Displacement diagram for C40 concrete (2%SP - 1%Fiber)

4.3.2.3 Mixture of 2% Super Plasticizer for – 1.5% Fibers

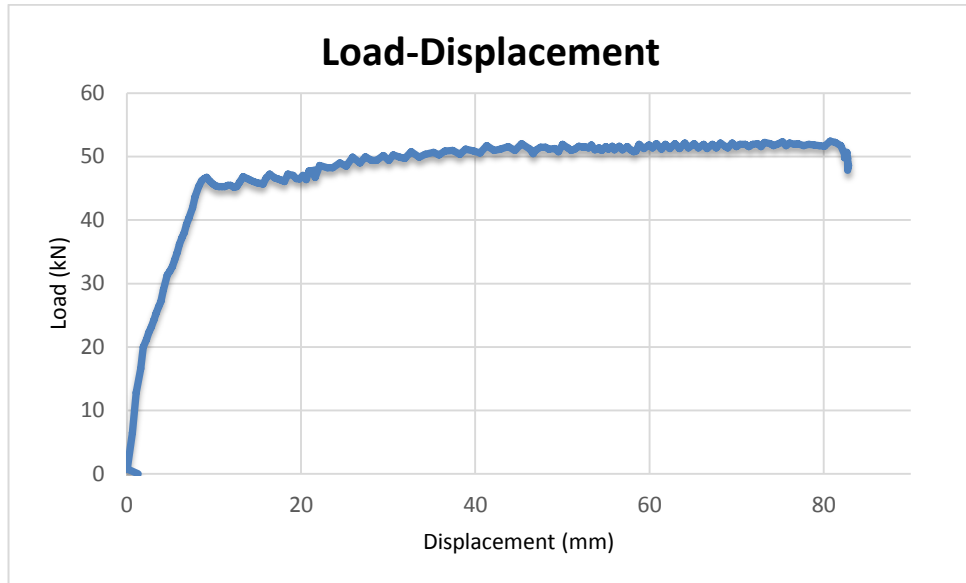


Figure 44: Load-Displacement diagram for C40 concrete (2%SP – 1.5%Fiber)

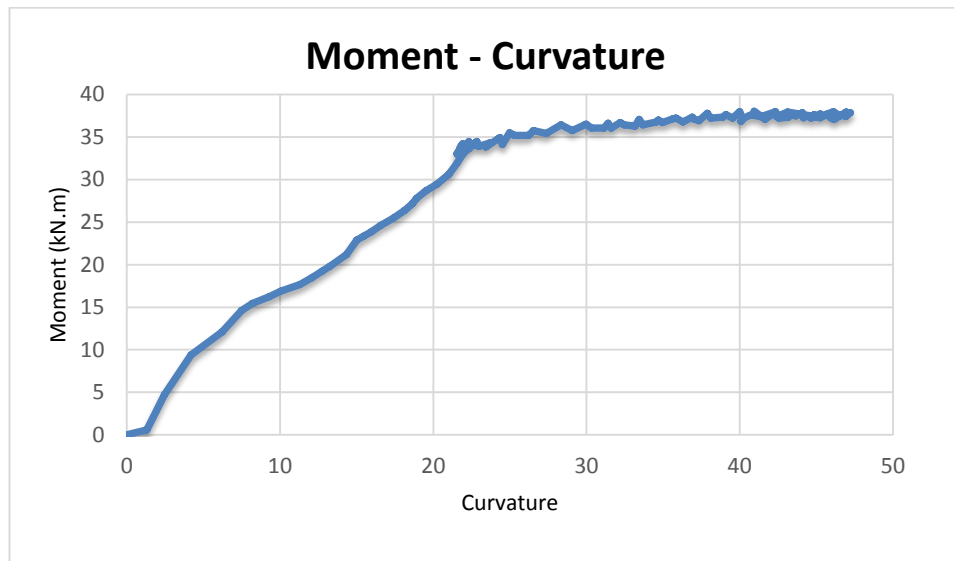


Figure 45: Load-Displacement diagram for C40 concrete (2%SP – 1.5%Fiber)

4.3.2.4 Mixture of 2% Super Plasticizer for – 2% Fiber

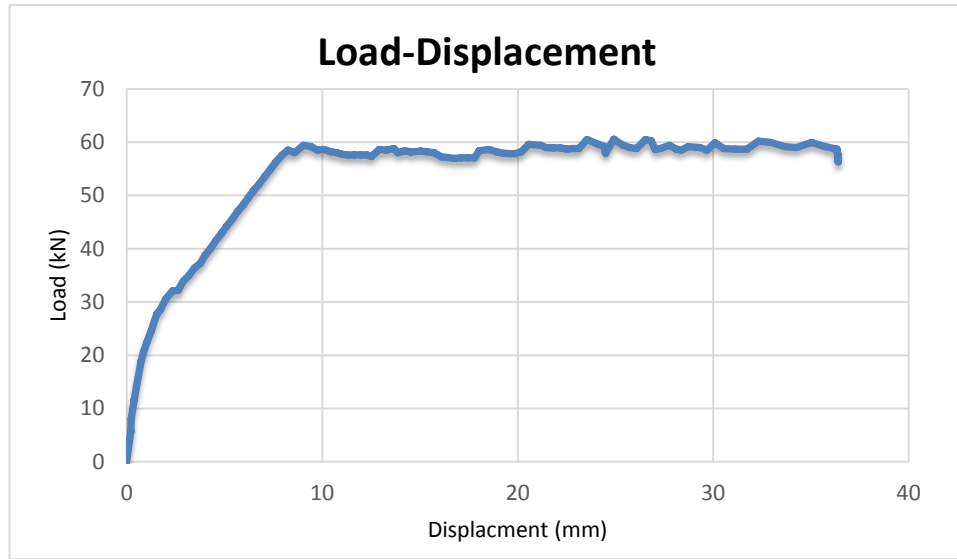


Figure 46: Load-Displacement diagram for C40 concrete (2%SP – 2%Fiber)

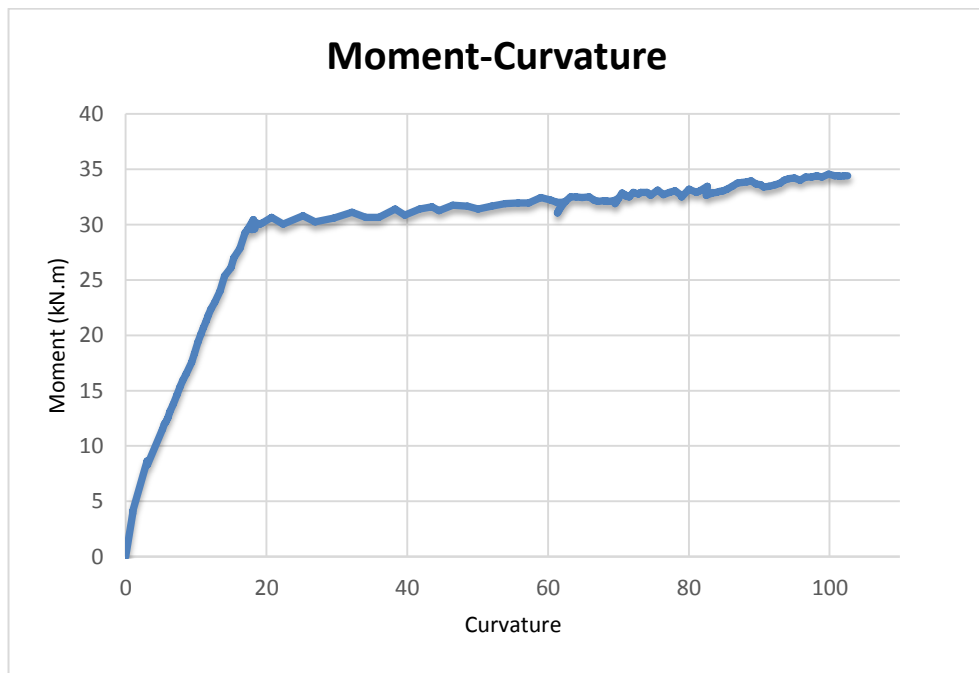


Figure 47: Moment-Curvature diagram for C40 concrete (2%SP – 2%Fiber)

4.3.2.5 Mixture of 1% Super Plasticizer for – 0% Fibers

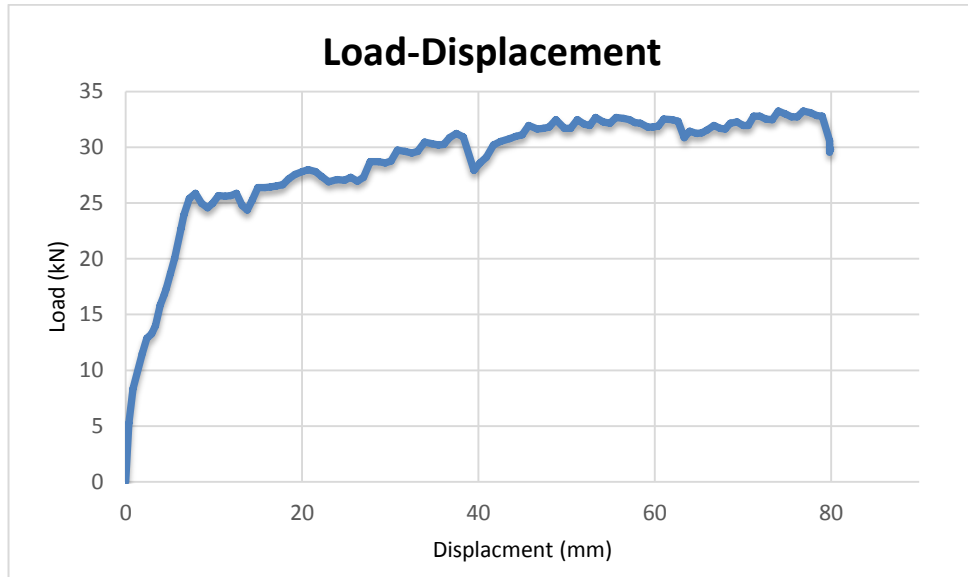


Figure 48: Load-Displacement diagram for C20 concrete (1%SP – 0%Fiber)

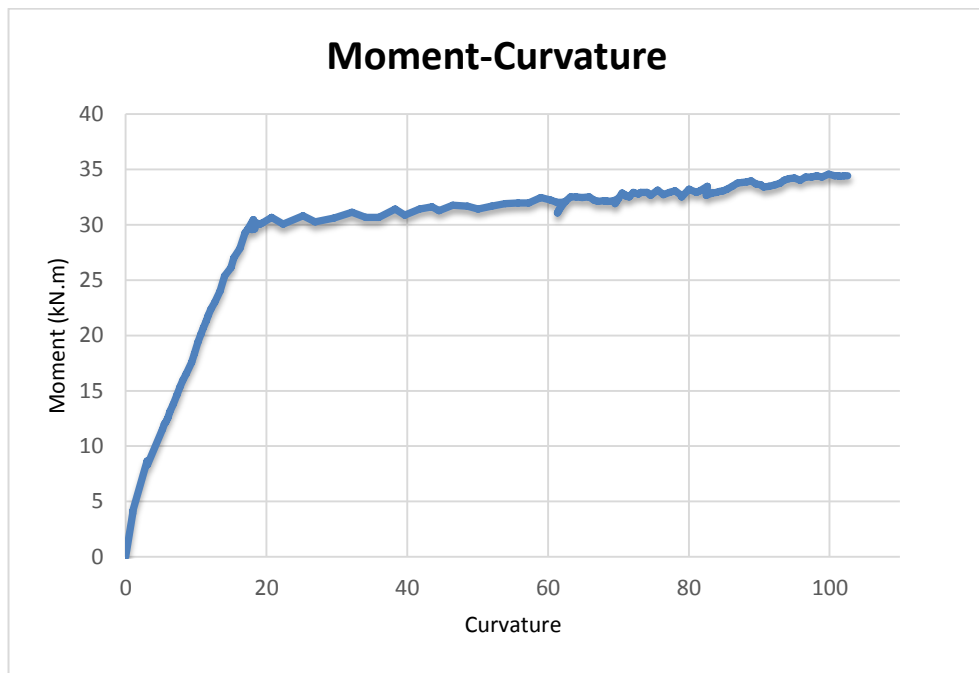


Figure 49: Moment-Curvature diagram for C20 concrete (1%SP – 0%Fiber)

4.3.2.6 Mixture of 1% Super Plasticizer for – 1% Fibers

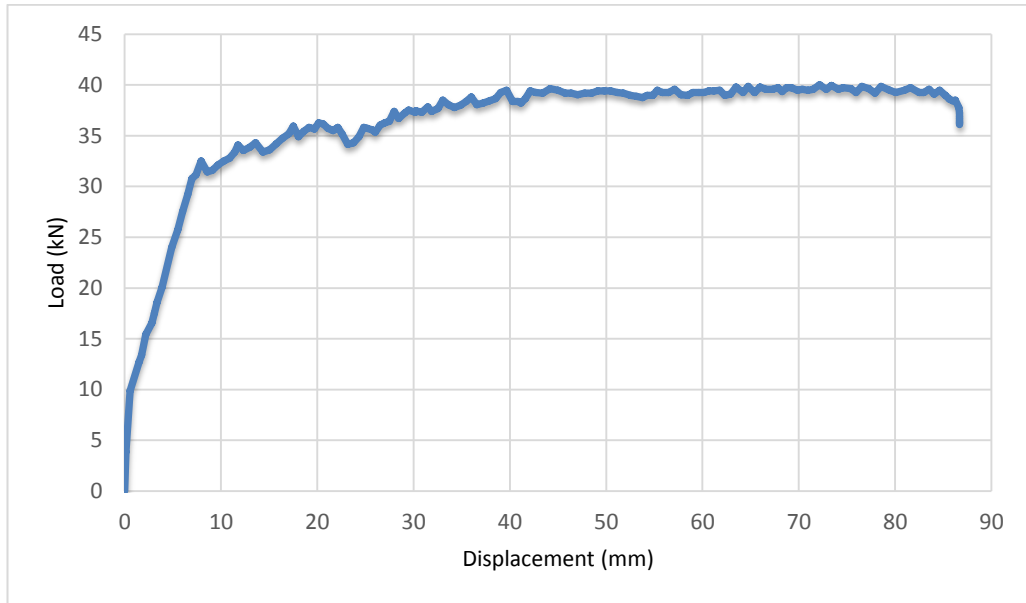


Figure 50: Load-Displacement diagram for C20 concrete (1%SP – 1%Fiber)

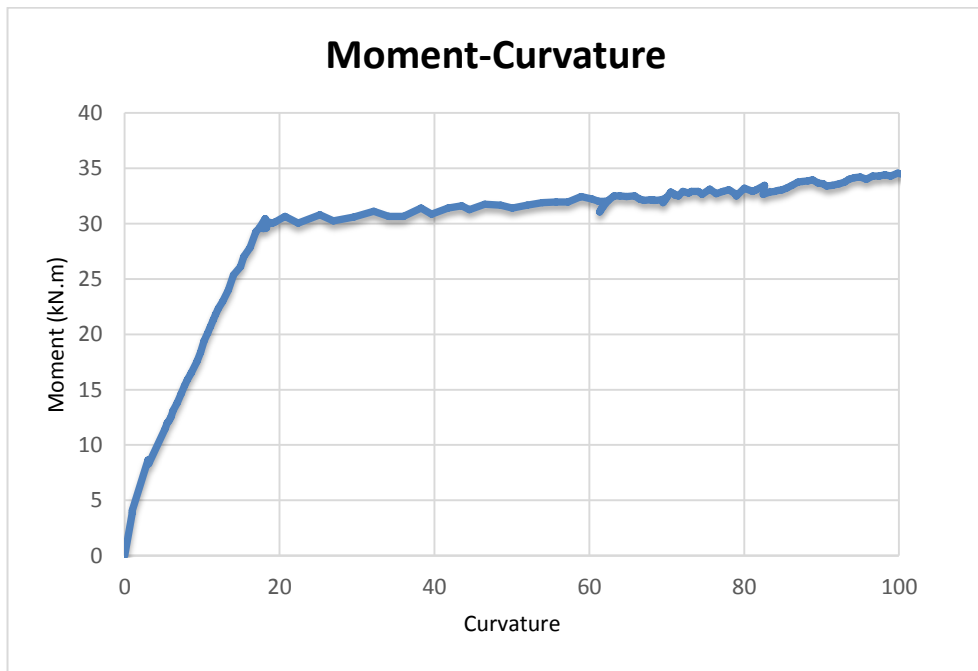


Figure 51: Moment-Curvature diagram for C20 concrete (1%SP – 1%Fiber)

4.3.2.7 Mixture of 1% Super Plasticizer for – 1.5% Fibers

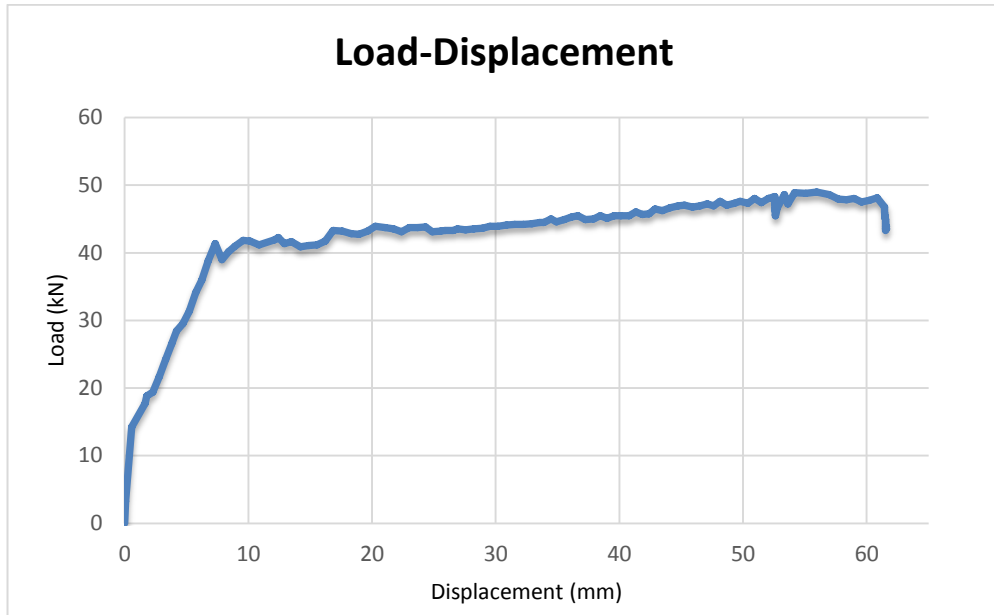


Figure 52: Load-Displacement diagram for C20 concrete (1%SP – 1.5%Fiber)

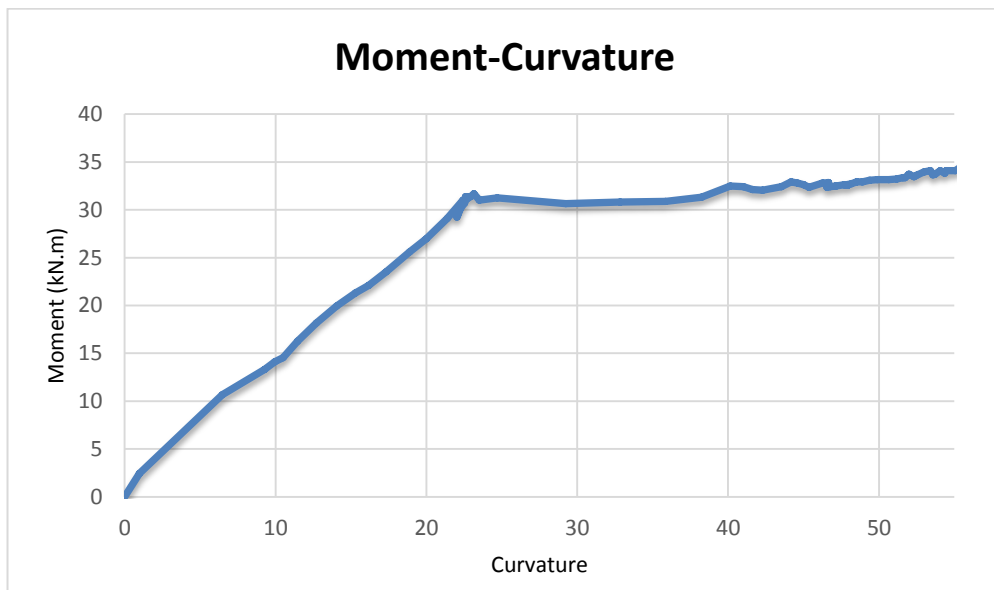


Figure 53: Moment-Curvature diagram for C20 concrete (1%SP – 1.5%Fiber)

4.3.2.8 Mixture of 1% Super Plasticizer for – 2% Fibers

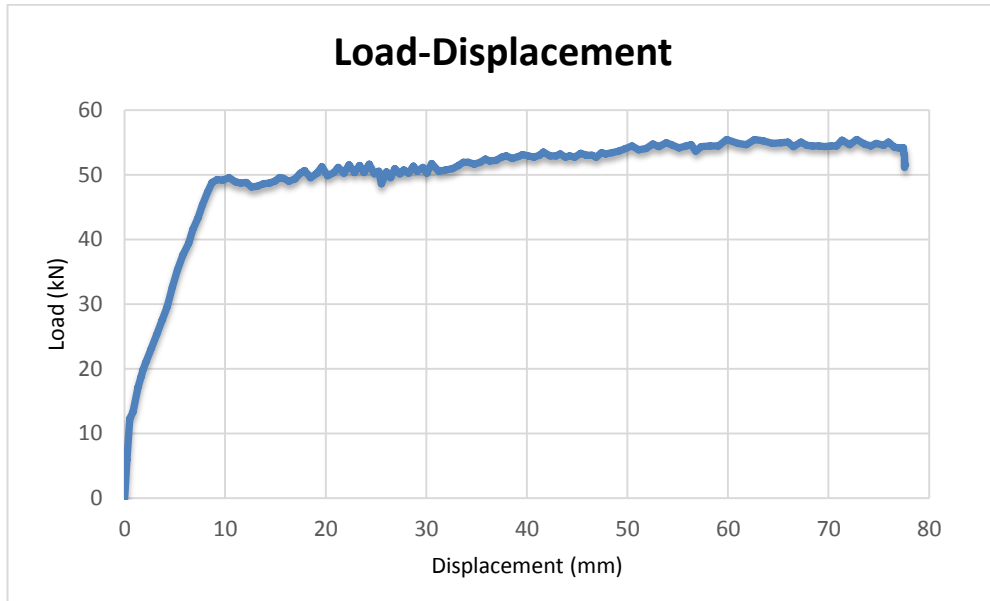


Figure 54: Load-Displacement diagram for C20 concrete (1%SP – 2%Fiber)

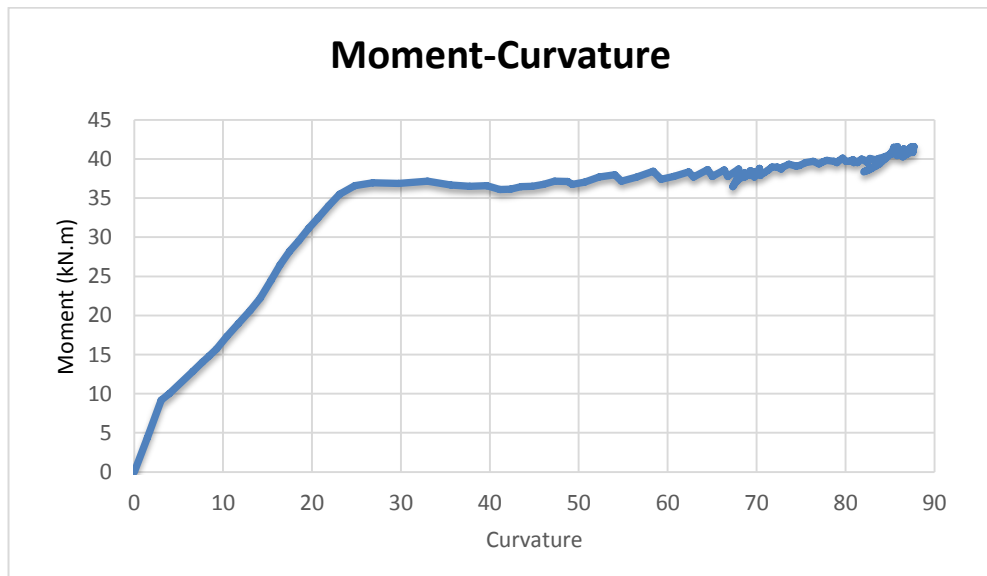


Figure 55: Moment-Curvature diagram for C20 concrete (1%SP – 2%Fiber)

4.3.2.9 Moment-Curvature Comparison of C20 and C40 Concrete

The below graphs show all sample behavior in moment-curvature, each slab contains two samples that represented the average. As can be seen, by increasing the percentage of fiber the amount of energy absorption increases and slabs can tolerant

more moment. In other words, fibers can change the behavior of slabs and make them more ductile. The beam with 2% fiber can tolerate more moment before cracking and save elastic mode. As can be seen on the graph below, the plain (0% fiber) slab can absorb less energy in comparison to the rest of the slabs.

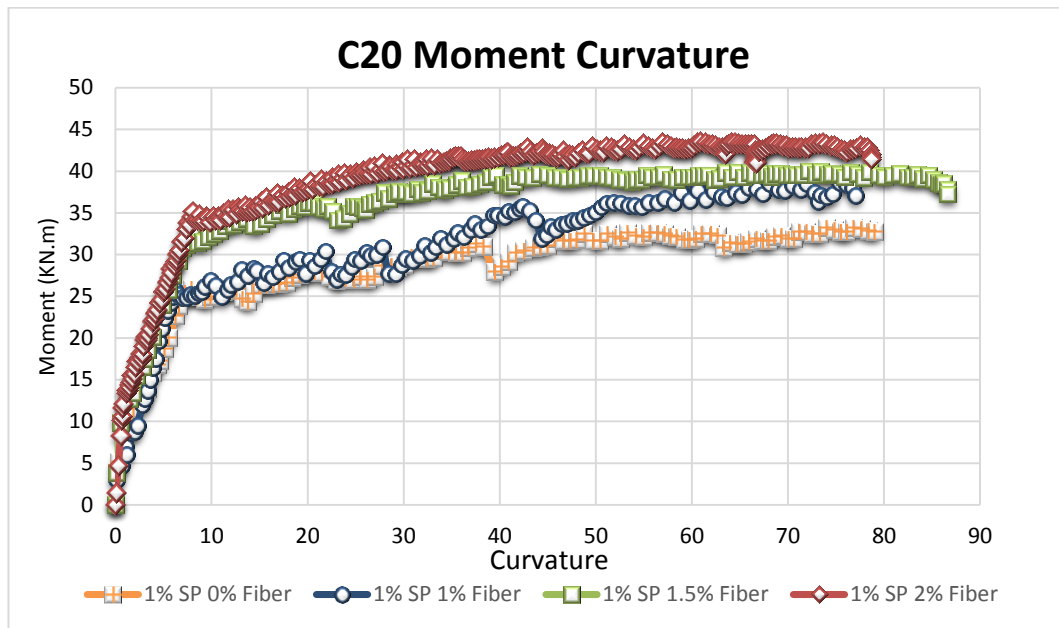


Figure 56: Moment-Curvature diagram C20

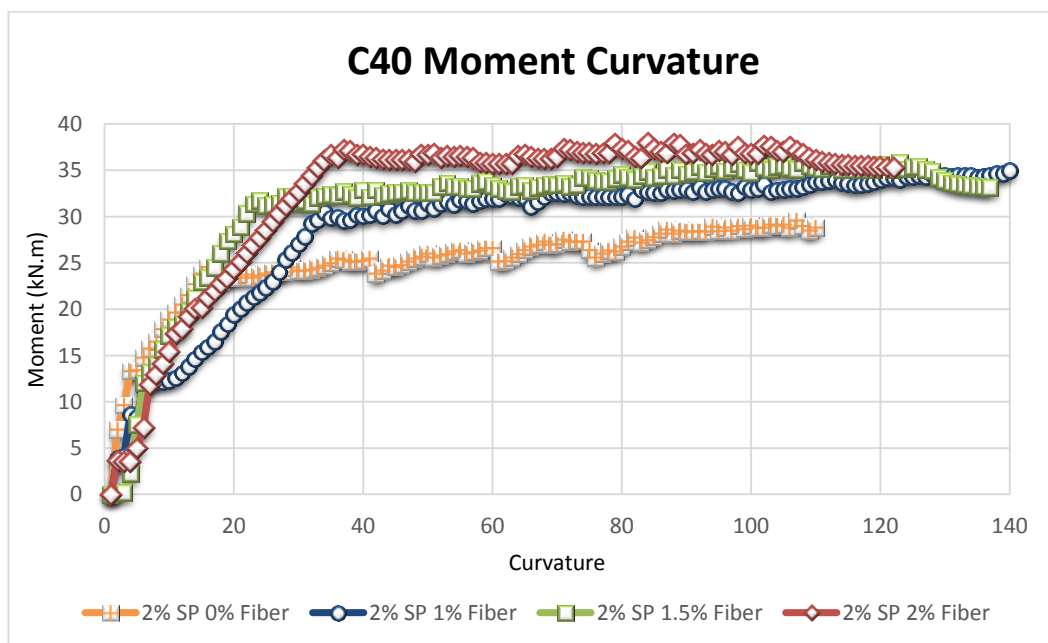


Figure 57: Moment-Curvature diagram C40

4.3.2.10 Load-Displacement Comparison of C20 and C40 Concrete

The below graphs show all sample behavior in Load-Displacement. As can be seen by increasing the percentage of fiber the amount of energy absorbing increase and slabs can tolerant more load. In other words, fibers can change the behavior and make slab more ductile.

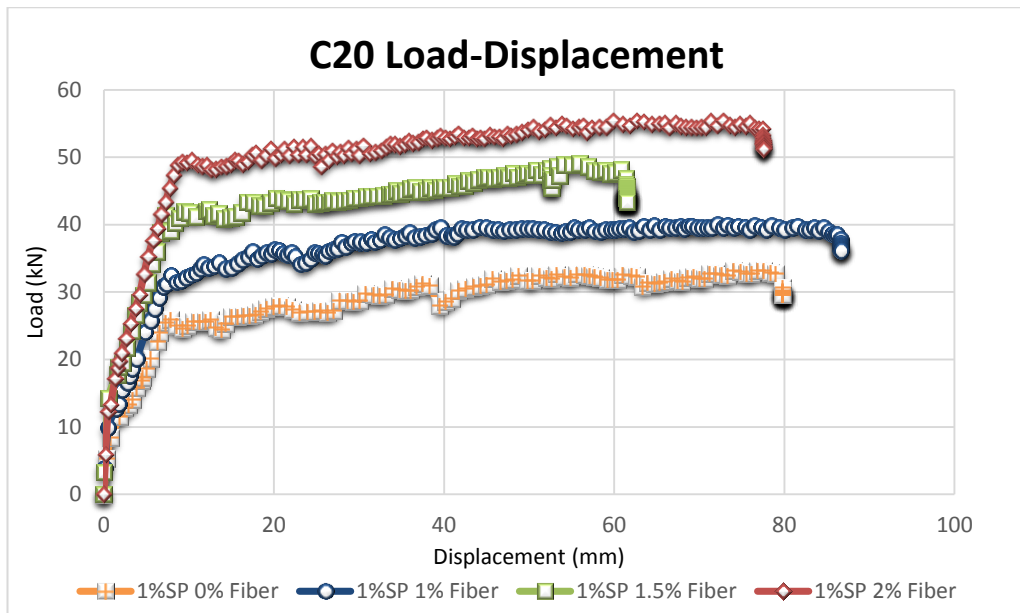


Figure 58: Load-Displacement diagram C20

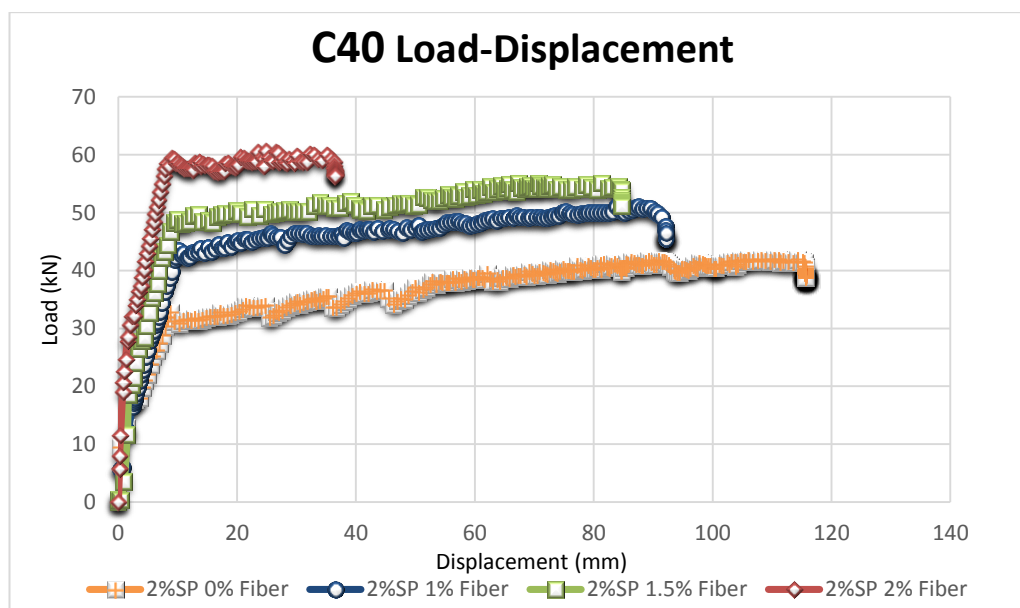


Figure 59: Load-Displacement diagram C40

4.3.2.11 Load-Displacement Behavior of C20 and C40 for Each Percentage of Fibers

The Figures from 60 to 63 compare the ductility behavior of C20 and C40 samples for different percentage of fibers. In the last section, the samples had been discussed according to the concrete class and the below diagrams are based on percentage of fibers. As can be seen, in Figures 60, 61 and 62 the ductility factor increased by increasing the compressive strength of concrete and in Figure 63 the C40 slab tolerant had been increased by absorbing the greater amount of energy but its ductility is less than C20. The energy absorptions according to concrete class and percentage of fibers are illustrated in Table 18.

Table 18: Energy absorption

Concrete Class	Fiber %			
	0.0%	1%	1.5%	2%
C20	2145.22*	2432.61	2650.32	3464.01
C40	4058.72*	4395.92	4756.59	1941.23

* The units are kN.mm

According to Table 18, both types of concrete have positive effects on the flexural stiffness and the energy absorption capacity. In the C20 slabs with 1%, 1.5% and 2% fiber have 13%, 23%, 61% improvement, respectively. In the C40 slabs with 1% and 1.5% fiber have 8% and 17% enhancements in energy absorption capacity, respectively. Compared to the slab without fiber, fibrous slab with 2% fiber in C20 and 1.5% fiber in C40 illustrate more efficient behavior for energy absorption capacity.

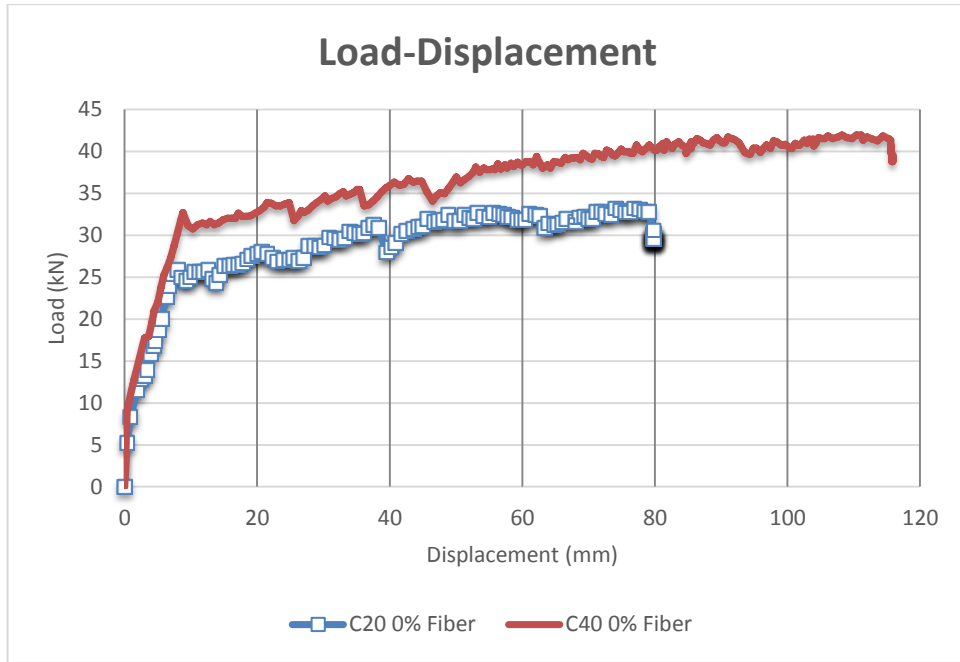


Figure 60: Load-Displacement diagram C20 and C40 0% Fiber

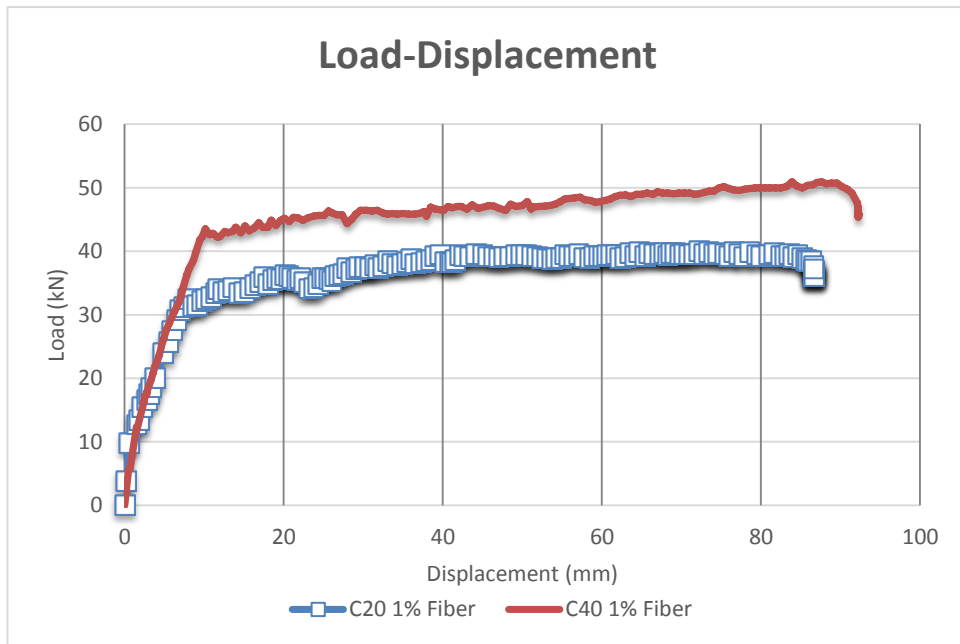


Figure 61: Load-Displacement diagram C20 and C40 1% Fiber

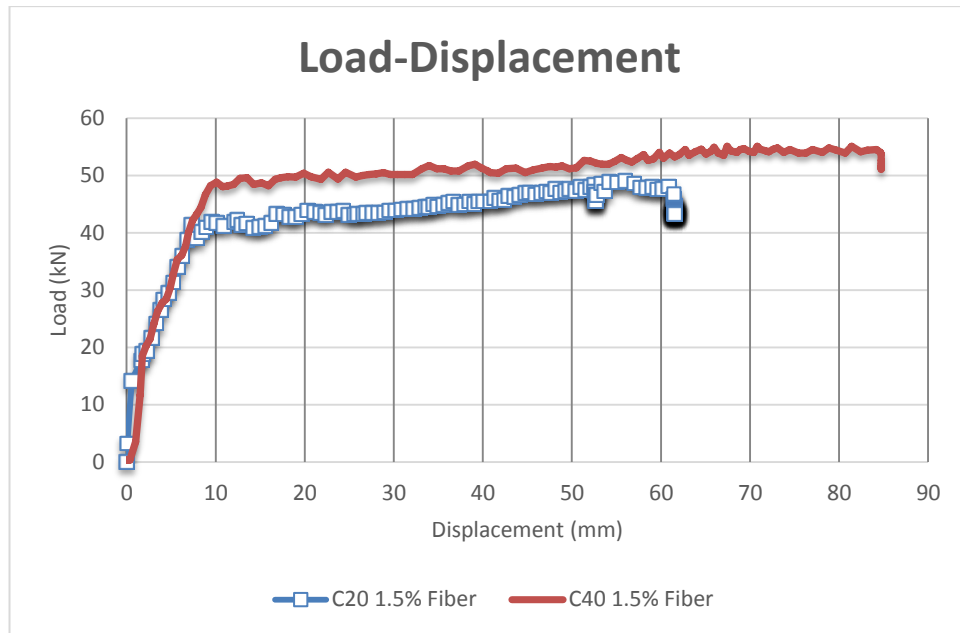


Figure 62: Load-Displacement diagram C20 and C40 1.5% Fiber

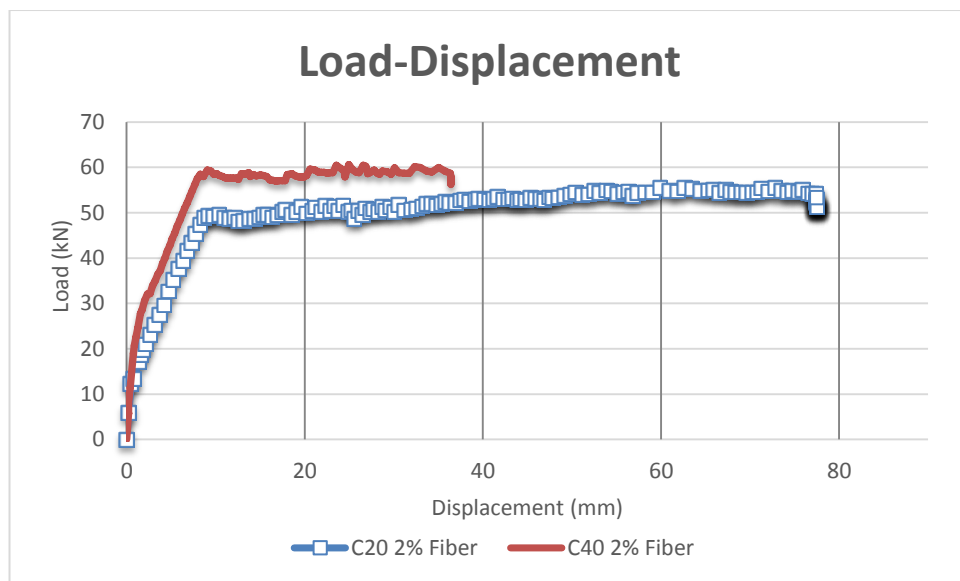


Figure 63: Load-Displacement diagram C20 and C40 2% Fiber

4.3.2.12 Stress Strain Relationship

For some problems occurred during tests, cubes were not tested for stress strain relationships. Instead cores were taken from each beams (totally 28 cores). The dimensions of each core were 65 mm diameter by 160 mm length (Figure 64). For this purpose two samples have been taken from two sides of beam beyond the

support which was placed during testing of beam and below results have been illustrated (Figures 65-66).



Figure 64: Core sample for Stress-Strain curvature

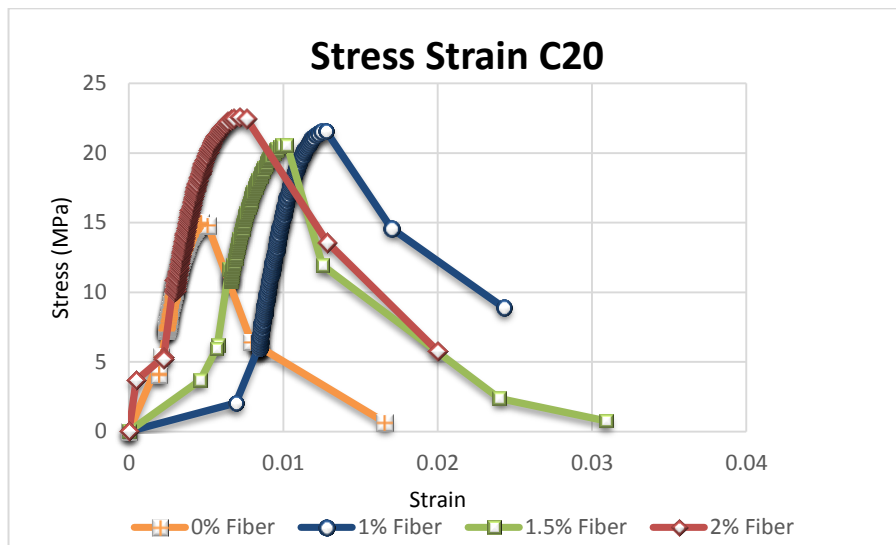


Figure 65: Stress-Strain curvature for C20

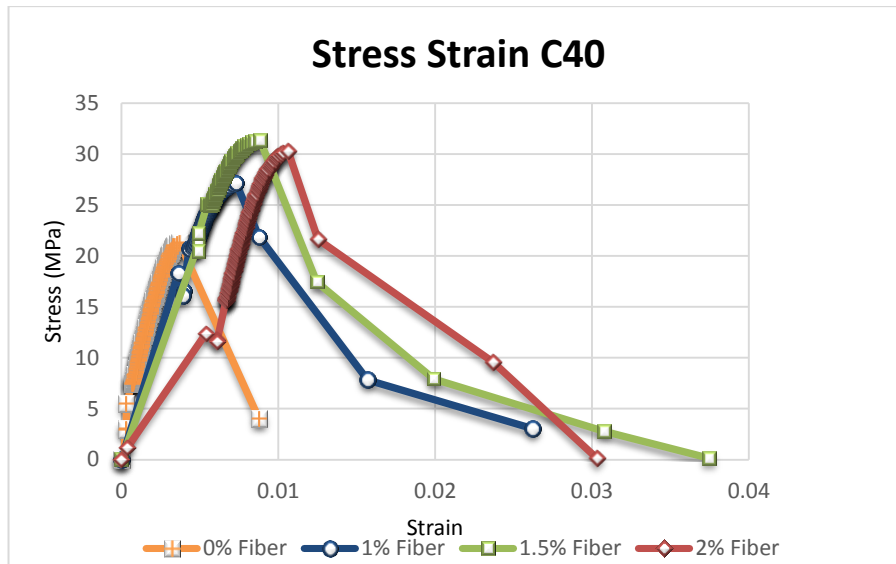


Figure 66: Stress-Strain curvature C40

Compression examinations of FRSCCs are illustrated in Figures 65 and 66. According to test results, by increasing in fiber percentage, the post-cracking compressive performance has been enhanced with 2% fibers in C20 and 1.5% fibers in C40. According to Figures 65 and 66, both types of mixes show an increase in strength by increasing the percentage of fibers in comparison to the plain samples. In the second graph (Figure 66), it is completely obvious that mix C40 has significant influence and this effect has been increased by increasing the percentage of fibers from 1% to 2%.

Fibers can improve the post-crack behavior and also enhance the amount of energy absorbing, as can be seen, the energy absorbing in the concrete of the classes of 40 is more than the other one. Also, fibers can influence on the tensile strength due to the bridging during crack Figure 67. Therefore, steel fibers in the reinforced concrete changed the behavior from brittle to ductile.



Figure 67: Fibers for bridging cracks

Chapter 5

CONCLUSION

5.1 Conclusions

In this chapter the significant results were reviewed and discussed briefly. The most effective role of fiber was to carry stress throughout the crack and then arrested the cracks opening and propagation. The ability of fiber to transform from a brittle concrete to a ductile was significant. It increased the energy absorption and strain capacity at peak load. Because of the interaction between fiber and concrete matrix, a crack section transferred a great part of tensile stresses which is called residual stresses.

According to the graphs in the last chapter, fiber affects the peak point load. By increasing the percentage of fiber in slab, this effect becomes more obvious. The peak point increase, related to the C20 slab with 2% fibers and the C40 slab with 2% fibers.

Results indicated that the absorption of energy increased significantly and the slabs ductility had been affected by increasing the concrete strength. As can be seen, in the Figures 60, 61 and 62 the ductility factor increased by increasing the compressive strength of concrete and in the Figure 63 the C40 slab tolerant had been increased by absorbing the greater amount of energy.

Figures 65 and 66 show C20 and C40 stress-strain relation which their strength was affected by fibers. Increasing in strength by increasing the percentage of fiber led to absorbing more energy and enhance the slabs toughness. Figure 66 shows more elastic behavior before peak load due to C40 and fibers influence.

Fibers can improve the post-crack behavior and also enhance the amount of energy absorbing, as can be seen, C40 can absorb the greater amount of energy. By comparing the two classes of concrete, it is clear the ductility can change by increasing the concrete strength.

5.2 Future Studies

This research can continue by using different type of fibers in size and compare them to the slab, which is modeled by the FEM analysis program to evaluate the differences between practical and theoretical.

REFERENCES

- ACI 301-99. (1999). *Specifications for Structural Concrete (ACI 301-99)*. American Concrete Institute.
- ACI Committee 237R-07. (2007). Self –consolidating concrete. *American concrete institute*, pp. 1-30.
- ACI Committee 544. (1990). State-of-the-art report on fiber reinforced concrete. *ACI manual of concrete practice*, Part 5; pp. 22.
- Alam, S. (2013). Principal Component and Multiple Regression Analysis for Steel Fiber Reinforced Concrete (SFRC) Beams. *International Journal of Concrete Structures and Materials*.
- Aslani, F. & Nejadi, S. (2013). Self-compacting concrete incorporating steel and polypropylene fibers: Compressive and tensile strengths, moduli of elasticity and rupture, compressive stress–strain curve, and energy dissipated under
ASTM C 136 – 06. (2006). Standard Test Method for Sieve Analysis of Fine and Coarse Aggregates. ASTM International.

ASTM C 1399-98. (2004) Test Method for Obtaining Average Residual-Strength of Fiber-Reinforced Concrete, *Annual Book of ASTM Standards*. Japan Society of Civil Engineers, Vol. 04.02.

ASTM C 1609/C 1609M – 05. (2006). Standard Test Method for Flexural Performance of Fiber-Reinforced Concrete (Using Beam With Third-Point Loading), *ASTM International*, PA, United States.

ASTM C39. (2014). *Standard Test Method for Compressive Strength of Cylindrical Concrete Specimens*. ASTM International.

Aydin, AC. (2007). Self compactability of high volume hybrid fiber reinforced concrete. *Constr Build Mater*; 21(6), pp. 1149–54.

Banthia, N. & Mindess, S. (2010). Toughness Characterization of Fiber Reinforced Concrete: Which Standard to Use. *ASTM, J. of Testing and Evaluation*, 32(2).

Banthia, N. & Trottier, J. (1994). Concrete reinforced with deformed steel fibres, part I: Bond-slip mechanisms. *ACI Materials Journal*, Vol. 91, No. 5, pp. 435-444.

Banthia, N. & Trottier, J.F. (1995). Test Methods of Flexural Toughness Characterization: Some Concerns and a Proposition, *Concrete Int.: Design & Construction, American Concrete Institute, Materials Journal*, 92(1), pp. 48-57.

Banthia, N. (2012). Fiber reinforced concrete.

Banthia, N. (2013). FRC: Milestone in international Research and development, proceedings of FIBCON2012, ICI, Nagpur, India, pp. 48.

Banthia, N., Gupta R. & Mindess, S. (1994). Developing crack resistant FRC overlay materials for repair applications, *NSF Conference, Bergamo, Italy*.

Barr, B., Gettu, R., Al-Oraimi, S.K.A. & Bryars, L.S. (1996). Toughness Measurements-the Need to Think Again, *Cement and Concrete Composites*, 18, pp. 281-297.

Barragan, B., Gettu, R., Cruz, C., Bravo, M. & Zerbino, R. (2005). Development and application of fiber-reinforced self-compacting concrete. In: Proceedings of the international conference on young researchers' forum, Thomas Telford Services Ltd, Dundee, Scotland, UK, pp. 165–72.

Brown, J. & Atkinson, T. (2013). Propex Concrete Systems (International), United Kingdom, proceedings of FIBCON2012, ICI, Nagpur, India.

Bui, V.K., Akkaya, Y. & Shah, S.P. (2002). Rheological model for self-consolidating concrete. *ACI Mater*, 99(6), pp. 549–59.

Campione, G. & Mangiavillano, M.L. (2008). Fibrous reinforced concrete beams in flexure: experimental investigation, analytical modelling and design considerations. *Eng Struct*, pp. 30:2970–80.

- Campione, G. (2008). Simplified flexural response of steel fiber-reinforced concrete beams. *ASCE J Mater Civil Eng*, pp. 20:283–93.
- Chanh, V. (2009). Steel fiber reinforced concrete.
- Chen, B. & Liu, J. (2000). Contribution of hybrid fibers on the properties of the control concrete hybrid fibers. *Cem. Con. Comp*, pp. 22(4): 343-351.
- Choi, K.K. & Park, H.G. (2007). Unified shear strength model for reinforced concrete beams-Part II: Verification and simplified method. *ACI Structural Journal*, 104(2), pp. 153–168.
- Collins, M.P. & Mitchell, D. (1991). Prestressed concrete structures. Englewood compression.Composites: Part B, 53, pp. 121–133.
- Cucchiara, C., Mendola, L. & Papia, M. (2004). Effectiveness of stirrups and steel fibres as shear reinforcement. *Cement and Concrete Composites*, Vol. 26, No. 7, pp. 777-786.
- Daczko, J. (2012). Self-consolidating concrete: hardened properties of SCC. New York, USA, ch. 4.
- Ding, Y., Liu, S., Zhang, Y. & Thomas, A. (2008). The investigation on the workability of fibre cocktail reinforced self-compacting high performance concrete. *Constr Build Mater*;22(7), pp. 1462–70.

- Ding, Y., Youb, Z. & Jalali, S. (2011). The composite effect of steel fibres and stirrups on the shear behaviour of beams using self-consolidating concrete. *Engineering Structures*, pp. 33 107–117.
- Ding, Y., Zhang, F., Torgal, F. & Zhang, Y. (2012). Shear behaviour of steel fibre reinforced self-consolidating concrete beams based on the modified compression field theory. *Composite Structures* 94, pp. 2440–2449.
- Edgington, J., Hannant, D. J. & Williams, R.I.T. (1978). Steel fibre reinforced concrete, fibre reinforced materials. Practical Studies from the Building Research Establishment, *The Construction Press, Lancaster*, pp. 112-128.
- EFNARC. (2002). Specification and guidelines for self-compacting concrete. European Federation of Supplies of Specialist Construction Chemicals, Farnham, Surrey, UK.
- Endgington, J., Hannant, D.J. & Williams, R.I.T. (1974). Steel fiber reinforced concrete. *Building research establishment Garston Watford*, pp CP 69/74.
- ENV 1992-1- 1. (1991). Eurocode 2: Design of concrete structures - Part 1: General rules and rules for buildings.
- Eren, O. & Alyousif, A. Production of self-compaction fiber reinforcement concrete in North Cyprus.

- Ezeldin, A. & Balaguru, P. (1989). Bond behavior of normal and high-strength fibre reinforced concrete. *ACI Materials Journal*, Vol. 86, No. 5, pp. 515-524.
- Fritih, Y., Vidal, T., Turatsinze, A. & Pons, G. (2013). Flexural and Shear Behavior of Steel Fiber Reinforced SCC Beams. *KSCE Journal of Civil Engineering*, pp.17(6):1383-1393.
- Frosch, R. J. (2000). Behavior of large-scale reinforced concrete beams with minimum shear reinforcement. *ACI Structural Journal*, Vol. 97, No. 6, pp. 814-820.
- Furlan, S. & Hanai, J. B. (1997). Shear behavior of fibre reinforced concrete beams. *Cement and Concrete Composites*, Vol. 19, No. 4, pp. 359-366.
- Gaimster, R. & Dixon, N. (2003). Self-compacting concrete. In *Advanced Concrete Technology*. Amsterdam: *Elsevier Butterworth-Heinemann*, pp. 9/1-9/21.
- Geiker, M. (2008). Self-compacting concrete (SCC). In *Developments in the formulation and reinforcement of concrete*. Cambridge: *Woodhead Publishing Limited*, pp. 187-207.
- Gopalaratman, V.S. (1991). Fracture Toughness of Fiber Reinforced Concrete, *ACI Materials Journal*. pp. 339-353, and Johnston, C.D., Discussion of above paper, *ACI Materials Journal*, pp. 304-309.

- Gribniak, V., Kaklauskas, G., Kwok Hung Kwan, A., Bacinskas, A. & Ulbinas, D. (2012). Deriving stress–strain relationships for steel fibre concrete in tension from tests of beams with ordinary reinforcement. *Engineering Structures*, pp. 42 387–395.
- Hammer, T.A. & Johansen, K. (2008). Influence of entrained air bubbles on matrix rheology. *To be presented at Nordic Concrete Research Projects 2005, Sandefford*.
- Hossain, K.M.A., Lachemi, M., Sammour, M. & Sonebi, M. (2013). Strength and fracture energy characteristics of self-consolidating concrete incorporating polyvinyl alcohol, steel and hybrid fibres. *Construction and Building Materials 45*, pp. 20–29.
- Johnston, C.D. (1974). Steel fiber reinforced mortar and concrete, A review of mechanical properties. *In fiber reinforced concrete ACI – SP 44*.
- Khayat, K.H. & Roussel Y. (2000). Testing and performance of fibre-reinforced self consolidating concrete. *Mater Struct*; 33(230), pp.391–7.
- Khuntia, M. & Stojadinovic, B. (2001). Shear strength of reinforced concrete beams without transverse reinforcement. *ACI Structural Journal*, Vol. 98, No. 5, pp. 48-56.

- Lachemi, M., Hossain, K.M.A., Lambros, V. & Bouzoubaä, N. (2003). Development of cost-effective self-consolidating concrete incorporating fly ash, slag cement, or viscosity-modifying admixtures. *ACI Mater*, 100(5), pp. 419–25.
- Lachemi, M., Hossain, K.M.A., Lambros, V. & Bouzoubaä, N. (2004). Self-compacting concrete incorporating new viscosity modifying admixtures. *Cem Concr Res*, 34(6), pp. 917–26.
- Lachemi, M., Sammour, M. & Sonebi, M. (2013). Strength and fracture energy characteristics of self-consolidating concrete incorporating polyvinyl alcohol, steel and hybrid fibres. *Construction and Building Materials* 45, pp. 20–29.
- Li, V.C., Ward, R. & Hamza, A. M. (1992). Steel and synthetic fibers as shear reinforcement. *ACI Materials Journal*, 89(5), pp. 499–508.
- Lim, D.H. & Oh, B.H. (1999). Experimental and theoretical investigation on the shear of steel fiber reinforced concrete beams. *Engineering Structures*, 21, pp. 937–944.
- Malhotra, V.M., Garette, G.G. & Bilodeau, A. (1994). Mechanical properties and durability of polypropylene fiber reinforced high-volume fly ash concrete for shotcrete applications. *ACI Mater*, 91(5), pp. 478–86.
- Mansur, M. A., Ong, K.C.G. & Paramasivam, P. (1986). Shear strength of fibrous concrete beams without stirrups. *ASCE Journal of Structural Engineering*, 112(9), pp. 2066–2079.

- Marini, A., Zanotti, C. & Plizzari, G. (2008). Seismic strengthening of existing structures by means of fibre reinforced concrete floor diaphragms. BEFIB.
- Mipenz, A (2001), Steel fibre reinforced concrete (SFRC) – Quality, performance and specification. BOSFA.
- Mirsayah, A. & Banthia, N. (2002). Shear strength of steel fiberreinforced concrete. *ACI Materials Journal*, Vol. 99, No. 5, pp.473-479.
- Mohammad, S., Islam, E. & Alam, S. (2013). Principal Component and Multiple Regression Analysis for Steel Fiber Reinforced Concrete (SFRC) Beams. *International Journal of Concrete Structures and Materials*.
- Naaman, A.E.(2003). Strain hardening and deflection hardening fiber reinforced cement composites. In: Naaman AE, Reinhardt HW, editors. International workshop high performance fiber reinforced cement composites. *RILEM Publications SARL*, pp. 95–113.
- Nanni, A. (1988). Splitting-tension test for fiber reinforced concrete. *ACI Mater* ,85(4), pp. 229–33.
- Narayanan, R. & Darwish, I.Y.S. (1987). Use of steel fibers as shear reinforcement. *ACI Structural Journal*, Vol. 84, No. 3, pp. 216- 226.
- Nataraja, M.C. (2011). Fiber reinforced concrete- behaviour properties and application. *Sri Jayachamarajendra College of engineering*.

- Nehdi, M. & Ladanchuk, JD. (2004). Fiber synergy in fiber-reinforced self-consolidating concrete. *ACI Mater*;101(6), pp. 508–17.
- Nemegeer, D., Vandewalle, L., Nieuwenburg, D., Van Gysel, A., Vyncke, J. & Deforche, E. (1995). Dramix guideline: Design of concrete structures - Steel wire fibre reinforced concrete structures with or without ordinary reinforcement, *Infrastructuur in het leefmilieu 4*, pp. 227-239.
- Oh, B. H. (1992). Flexural analysis of reinforced concrete beams containing steel fibres. *Journal of Structural Engineering*, Vol. 118, No. 10, pp. 2821-2836.
- Ozawa, K., Maekawa, K., Kunishima, H. & Okamura H. (2013). Performance of concrete based on the durability design of concrete structures. In: Proc of the second east-Asia-pacific conference on structural engineering and construction, Bangkok, Thailand, vol. 1. pp. 445–56.
- Pir, A. (2013). Experimental and Numerical Investigation on Steel Fibrous Reinforced Concrete Slab Strips with Traditional Longitudinal Steel Bars. Master thesis.
- Portable data logger, TDS-303. Tokyo Sokki Kenkyujo.
- Radtke, F.K.F., Simone, A. & Sluys, L.J. (2010). A computational model for failure analysis of fibre reinforced concrete with discrete treatment of fibres. *Eng Fract Mech*, pp. 77:597–620.

- Ramakrishna, G. & Sundararajan, T. (2005). Studies on the durability of natural fibres and the effect of corroded fibres on the strength of mortar. *Cement & Concrete Composites*, 27(5), pp. 575–582.
- Rols, S., Ambroise, J. & Pera, J. (1999). Effects of different viscosity agents on the properties of self-leveling concrete. *Cem Concr Res*, 29(2), pp. 261–6.
- Ruano, G., Isla, F., Pedraza, R., Sfer, D. & Luccioni, B. (2014). Shear retrofitting of reinforced concrete beams with steel fiber reinforced concrete. *Construction and Building Materials*, pp. 54 646–658.
- Sahmaran, M., Yurtseven, A. & Ozgur YI. (2005). Workability of hybrid fibre reinforced self-compacting concrete. *Build Environ*; 40(12), pp. 1672–7.
- Sarmiento, E. (2011). Influence of concrete flow on the mechanical properties of ordinary and fiber reinforced concrete. Technical University of Catalonia (UPC). MS thesis.
- Shetty, M. (2005). *The concrete technology, theory and practice*. New Delhi: S. Chand and Company LTD.
- Shin, S. W., Oh, J. G. & Ghosh, S. K. (1994). Shear behavior of laboratory-sized high strength concrete beams reinforced with bars and steel fibers. *American Concrete Institute, Special Publication*, Vol. 142, No. 10, pp. 181-200.

- Soltanzadeh1, F., Mazaheripour, H., Barros, J. & Sena, J. (2013). Shear Capacity of HPFRC Beams Flexurally Reinforced with Steel and Prestressed GFRP Bars. FRPRCS-11 Joaquim Barros & José Sena-Cruz (Eds) UM, Guimarães.
- Tlemat, H., Pilakoutas, K. & Neocleous, K. (2003). Pullout behaviour of steel fibers recycled from used tires. In: Role of concrete in sustainable development, pros of instep on celebrating concrete: people and practice, Thomas Telford Ltd., Dundee, pp. 175–84.
- Turatsinze, A., Granju, J. L, Sabathier, V. & Farhat, H. (2005). Durability of bonded cement-based overlays: Effect of metal fibre reinforcement. *Materials and Structures*, Vol. 38, No. 3, pp. 321- 327.
- Vandewalle, L. (2000). Cracking behaviour of concrete beams reinforced with a combination of ordinary reinforcement and steel fibers. *Materials and Structures/Materiaux et Constructions*, pp. 164-170.
- Vecchio, F.J. & Collins MP. (1986).The modified compression field theory for reinforced concrete elements subjected to shear. *American Concrete Institute*, pp. 83(2):219–31.
- Vikrant, S., Vairagade, K. & Kene, S. (2012). Introduction to Steel Fiber Reinforced Concrete on Engineering Performance of Concrete. *International Journal of Scientific & Technology Research*, Volume 1, Issue 4.

Yakhlaf, M. (2013). Development of Carbon Fiber Reinforced Self-Consolidating Concrete Patch for Repair Applications. The University of Waterloo. Master thesis.

